81-2242

1980 Annual Report: Technical Assistance for Future Insulation Systems Research

R. J. Van Brunt, M. Misakian, and D. A. Leep

Electrosystems Division
U.S. Department of Commerce
National Bureau of Standards
Washington, DC 20234

K. J. Moy, Graduate Student

University of California

E. C. Beaty

Quantum Physics Division
U.S. Department of Commerce
National Bureau of Standards
Boulder, CO 80303

January 1981

Issued April 1981

ored by
e of Electric Energy Systems
rtment of Energy

NBSIR 81-2242

1980 ANNUAL REPORT: TECHNICAL ASSISTANCE FOR FUTURE INSULATION SYSTEMS RESEARCH

R. J. Van Brunt, M. Misakian, and D. A. Leep

Electrosystems Division
U.S. Department of Commerce
National Bureau of Standards
Washington, DC 20234

K. J. Moy, Graduate Student

University of California

E. C. Beaty

Quantum Physics Division
U.S. Department of Commerce
National Bureau of Standards
Boulder, CO 80303

January 1981

Issued April 1981

Sponsored by
Office of Electric Energy Systems
Department of Energy

U.S. DEPARTMENT OF COMMERCE, Malcolm Baldrige, *Secretary*
NATIONAL BUREAU OF STANDARDS, Ernest Ambler, *Director*

TABLE OF CONTENTS

Abstract

An experimental technique has been developed to quantify the electrical characteristics of pulse-type partial discharges (corona) in compressed electronegative gases. By this method the pulse repetition rates, shapes, and height distributions are determined together with the average current. The technique has been applied to the investigation of corona behavior in compressed SF_6 and SF_6/N_2 mixtures, and to measurements of corona inceptions in SF_6 for both dc and 60-Hz ac voltages. A gas chromatograph-mass spectrometer has been employed to monitor production of trace contaminants by corona-induced degradation of SF_6. The most abundant gaseous by-products that were detected from dc corona were H_2O, SOF_2, and SO_2F_2. The results of chemical analysis were correlated with measurements of the electrical characteristics of the corona. It was discovered that the pulse height distributions and repetition rates were sensitive to the presence of trace contaminants at the ppm level. Experiments were also performed on the effect of trace levels of water vapor, introduced by heating a wire, on positive dc corona pulse burst behavior in SF_6. It was noted that the burst activity was significantly inhibited by trace amounts of H_2O. These results indicate that measurement of pulse characteristics of positive corona can be used as a sensitive monitor of gaseous contamination levels. The effects of uv radiation and optical radiation from a tunable dye laser on electrical behavior of corona in SF_6 and N_2 were investigated. Ultra-violet light can have, under certain conditions, a large effect on initiation of electron avalanches in SF_6 near onset. Optical radiation in the wavelength range 580 to 620 nm

was found to produce a measurable effect on corona in N_2 when it impinged on the electrode surfaces. A bibliography of electron swarm data needed to predict theoretically breakdown and to model discharge phenomena in gases was prepared.

Disclaimer:

This is a report of an ongoing research project. Therefore, some of the results presented here, although believed to be correct, must still be considered preliminary. The conclusions based on the data given in this report must also be viewed as tentative and subject to possible revisions as additional information is acquired.

Summary

Progress was made on the development of new measurement methods to study fundamental physical and chemical properties of partial discharges (corona) in SF_6 and other gaseous dielectrics. A fast multichannel analyzer system was adapted to the measurement of point-plane corona pulse characteristics. The electrical properties of corona pulses, which include pulse height distributions, pulse repetition rates, pulse shapes, and average corona current, were measured for SF_6 and SF_6/N_2 mixtures as a function of gas pressure, composition, applied voltage, and polarity. The measurement system was used for investigations of corona inception voltages for dc and 60-Hz ac conditions in compressed SF_6. The results of inception voltage measurements indicate that observations made under dc conditions cannot always indicate what will happen for 60-Hz ac. At pressures above 200 kPa ($\sim$2 atm) the effects of field enhancement due to space charge in the gap become significant in determining positive inception under ac conditions. The effects of uv radiation on measurement of SF_6 corona inception under ac and dc conditions were also examined. For some conditions of gas pressure and gap spacing, uv radiation was found to have a very large effect on the probability of electron avalanche development near onset. This is particularly true for positive dc corona.

A gas chromatograph-mass spectrometer system was used to analyze the content of SF_6 which had been subjected to continuous low level positive corona for extended periods of time (up to 333 hours). The most abundant end decomposition products that were identified are H_2O, SOF_2, and SO_2F_2. Quantitative analysis of the latter two species has been possible, whereas the

H_2O content could only be determined on a relative scale. The H_2O appears to arise from heating of the electrodes by action of the discharge and thus its presence at trace levels is difficult to avoid. After 24 hours of corona at the 2.0 μA level, SOF_2 and SO_2F_2 were found to be present at roughly the 10 and 30 ppm levels respectively. These arise from reactions of the primary decomposition products, namely lower valence sulfur fluorides, with H_2O. These reactions also lead to production of HF.

The results of chemical analysis were correlated with measurements of the electrical characteristics of the corona. It was found that discernible changes in the positive corona pulse repetition rates and pulse height distributions occurred after only a few hours of continuous corona. The burst characteristics of positive dc corona in SF_6 seem to be quite sensitive to trace levels of polar contaminants such as H_2O. This was verified in experiments where trace amounts of H_2O were introduced into the gas by heating a wire, i.e., via thermally-induced desorption from a surface. The presence of H_2O and, by inference, other polar molecules appears to inhibit pulse burst development. This behavior is believed to be related to the effect these molecules have on the dynamics of positive ion space charge in the gap. The results of this study imply that positive corona pulse height distributions are sensitive indicators of gaseous contamination. The information obtained here should help in the design of future tests to determine relative performance of various gaseous dielectrics with respect to dielectric strength and long-term stability under electrical stress.

Attempts were made to observe the optogalvanic effect in N_2 corona discharges using coaxial electrodes and a tunable dye laser which could be

operated between 580 and 620 nm. Although no optogalvanic signals were observed when the laser beam passed through the gas, the corona current was affected by light impinging on the electrode surfaces. The physical basis for this effect is not yet understood, but it might prove to be a useful probe of surface conditions.

A bibliography of electron swarm data needed to predict breakdown and to model discharge phenomena in gases was prepared. A compilation of swarm data with critical evaluation is near completion.

I. Introduction

The objective for this project is to develop diagnostic techniques for monitoring, identifying, and predicting degradation in future compressed gas electrical insulating systems under normal operating conditions. The focus is on providing fundamental information and data needed to improve test design and performance evaluation criteria. The major emphasis has been on a laboratory study of partial discharge (corona) phenomena in gaseous dielectrics. The research effort reported here has been concerned with 1) characterization of corona phenomena under dc and 60-Hz ac conditions, 2) monitoring of corona-induced chemical changes in gaseous insulation, and 3) obtaining fundamental data needed to model and predict discharge inception and corona behavior. A compilation and critical evaluation of existing fundamental electron swarm data for electronegative gases has been underway.

Because of the importance and prevalence of corona in practical high voltage systems, there is need to better understand this phenomenon and the effect it can have on system performance. There is particular concern about the degradation that can result if the insulation system is subjected to continuous corona for an extended period of time. Not only can the insulating qualities of the gas deteriorate as the result of corona, but also highly toxic substances might be produced which could be a hazard to human health and safety if released into the environment.

It is desirable to know the effect that gaseous contaminants can have on dielectric strength and corona discharge characteristics such as inception voltage, current growth, discharge pulse rates, and pulse height distributions. An understanding of the fundamental mechanisms that determine corona discharge

characteristics and eventual breakdown would be useful in the design of improved gaseous dielectrics, and in devising physically meaningful and relevant tests of dielectric performance. In the measurement and observation of corona phenomena in gaseous insulation, there is the need for improved measurement methods that can be used in the laboratory to meaningfully quantify corona characteristics in a reproducible way so that results obtained in one laboratory can be directly compared to results from another. Much of the early research on corona phenomena has produced an abundance of qualitative information which, although interesting, is often of limited usefulness. The question of defining partial discharge inception in compressed electronegative gases for different voltage waveforms needs to be addressed. In considering the problem of corona inception it is necessary to understand the statistics of electron avalanche initiation and growth. A model to predict electron avalanche statistics may also prove to be a useful way to predict time-to-breakdown in practical systems that are locally overstressed.

In developing models to predict breakdown, corona inception, and electron avalanche statistics, it is necessary to understand the basic ionization processes that occur in a gas. In particular, it is necessary to have reliable, fundamental electron swarm data such as electron drift velocities, electron kinetic energy distributions and electron ionization, attachment, and detachment rates. Progress in the theoretical modeling of discharge phenomena can be greatly hindered by the lack of good swarm data. Often reliable swarm data in electronegative gases cannot be obtained by traditional measurement methods, and must instead be generated from data on electron collision cross sections. There is a clear need for the generation, compilation and

evaluation of electron swarm data in support of future modeling efforts. There is also a need for a more thorough compilation and evaluation of electrical breakdown data in gases. This data is not only needed by those involved with design of future high voltage insulating systems, but also by those who want to test theoretical models to predict breakdown.

During the past year research was conducted at NBS to meet the objectives discussed above. The problems of measuring and defining corona inception in SF_6 were addressed. Measurements were made of corona inception voltages for compressed SF_6 under both dc and 60-Hz ac conditions. A model was proposed to explain observed differences between the ac and dc results.[1] The effects of uv radiation on corona discharge inception and electron avalanche initiation were also examined for both ac and dc conditions.

A technique to measure pulse height distributions of partial discharges in gases as a means of statistically quantifying the discharge activity was evaluated. A system has been devised to determine the electrical characteristics of pulse-type corona which includes measurement of pulse shapes, pulse repetition rates, pulse amplitude distributions, as well as average corona current. Electrical characteristics of positive and negative dc corona in SF_6 and SF_6-N_2 mixtures have been measured and the results reported.[2]

A gas chromatograph-mass spectrometer (GC/MS) system has been developed and calibrated for use in sensitive monitoring of trace contaminants and decomposition products in gaseous dielectrics. The instrument can presently be used for quantitative analysis to the ppm level of some of the more important decomposition products in SF_6. It has been used to identify and measure

build-up of decomposition products in SF_6 produced by continuous positive dc corona. A hot wire technique was developed and tested for artificially introducing trace amounts of water vapor into compressed SF_6 which could be monitored using the GC/MS. The effects of trace levels of corona-induced decomposition products as well as artificially introduced H_2O on the electrical characteristics of dc corona in SF_6 have been investigated and reported.[3] An investigation of the effects of an intense tunable laser beam on development of dc corona discharges in N_2 was also carried out.

A program to compile and evaluate electron swarm data relevant to high-voltage insulation research has been formulated and discussed[4] and a comprehensive bibliography of electron swarm data has been prepared.[5] Serious consideration is now being given to setting up a data center to collect, evaluate and disseminate electrical breakdown data for gases.

In other activities related to this research, a report[6] was prepared containing the minutes of the Workshop on Gaseous Dielectrics for Use in Future Electric-Power Systems which was held at the National Bureau of Standards on September 10-11, 1979. This meeting was sponsored jointly by the Department of Energy, National Bureau of Standards, and the Electric Power Research Institute and held for the purpose of discussing technological barriers to the development and use of new gaseous insulation. A report[7] was also prepared on the safe handling of SF_6 for use in high voltage electrical apparatus. This report was primarily for the benefit of those at NBS who must work with this material in the laboratory.

II. Technical Progress

II.A. Characterization of Corona Pulses in SF_6 and SF_6 - N_2 Mixtures

II.A.1 Motivation

Until very recently there has been, in general, a lack of information on the fundamental properties of corona in pressurized SF_6 and other electronegative gases, excluding, of course, air. This fact has previously been noted in the literature.[8,9] There is also a need to be more quantitative in the description of corona phenomena. It is known from previous studies that dc corona in SF_6, at pressures above 50 kPa, occurs predominantly in the form of pulse bursts from inception to breakdown.[9-11] A complete quantitative electrical description of this phenomenon, which is statistically useful, would require information on distribution of pulse shapes and pulse heights, pulse burst length, repetition rates and the relationship of these to the observed total average corona current at a given applied voltage, gas pressure, and electrode configuration.

As a first step in quantifying the corona activity we have, in this work, placed emphasis on the problem of measuring the pulse height distribution (PHD) characteristic using a fast multichannel analyzer (MCA). With this system the electrical characteristics of dc corona in SF_6 and SF_6/N_2 mixtures have been measured under a variety of conditions of gas mixture, total pressure, and applied voltage using a point-plane electrode system. Preliminary results of these measurements have already been reported.[2]

It should be noted that the pulse height analysis technique for observing partial discharges is not new. It has been applied in previous work to monitor degradation in insulating materials.[12-15] The technique, however, has met

with only limited success thus far, due mainly to difficulties associated with interpretation of the results. The physical basis for changes in PHD's with time under stress has not been well understood. To our knowledge there have been no attempts to apply this technique to fundamental characterization of partial discharges in electronegative gases.

II.A.2 Apparatus

For these measurements, corona was generated by applying high voltage to a cell containing point-plane electrodes. Using the standard convention, the polarity of the corona refers to the polarity of the voltage applied to the stressed electrode, namely the point. A schematic giving essential features of the system used for these investigations is shown in Fig. 1. More details of the multichannel analyzer system have been given in an earlier report[16] and will not be discussed here. It should be noted however that some modification of the instrument as described in Ref. 16 was necessary for the study of gas discharges.

In pointing out the essential features, we note that the system can be used to measure either 60-Hz ac or positive and negative dc partial discharges. For ac measurements a gating arrangement is employed to control the phase interval of observation. Using this it is possible to measure separately ac positive and negative partial discharge inceptions. The pulse rate of the partial discharges is measured with a gated scaler for both ac and dc voltages. The PHD's are measured with a multichannel analyzer (MCA) the input of which is a peak-and-hold circuit. The peak-and-hold circuit is designed to detect the peak of a pulse in a time interval of 2 μs once the input voltage exceeds a level determined by a discriminator. The dead time (minimum sampling interval)

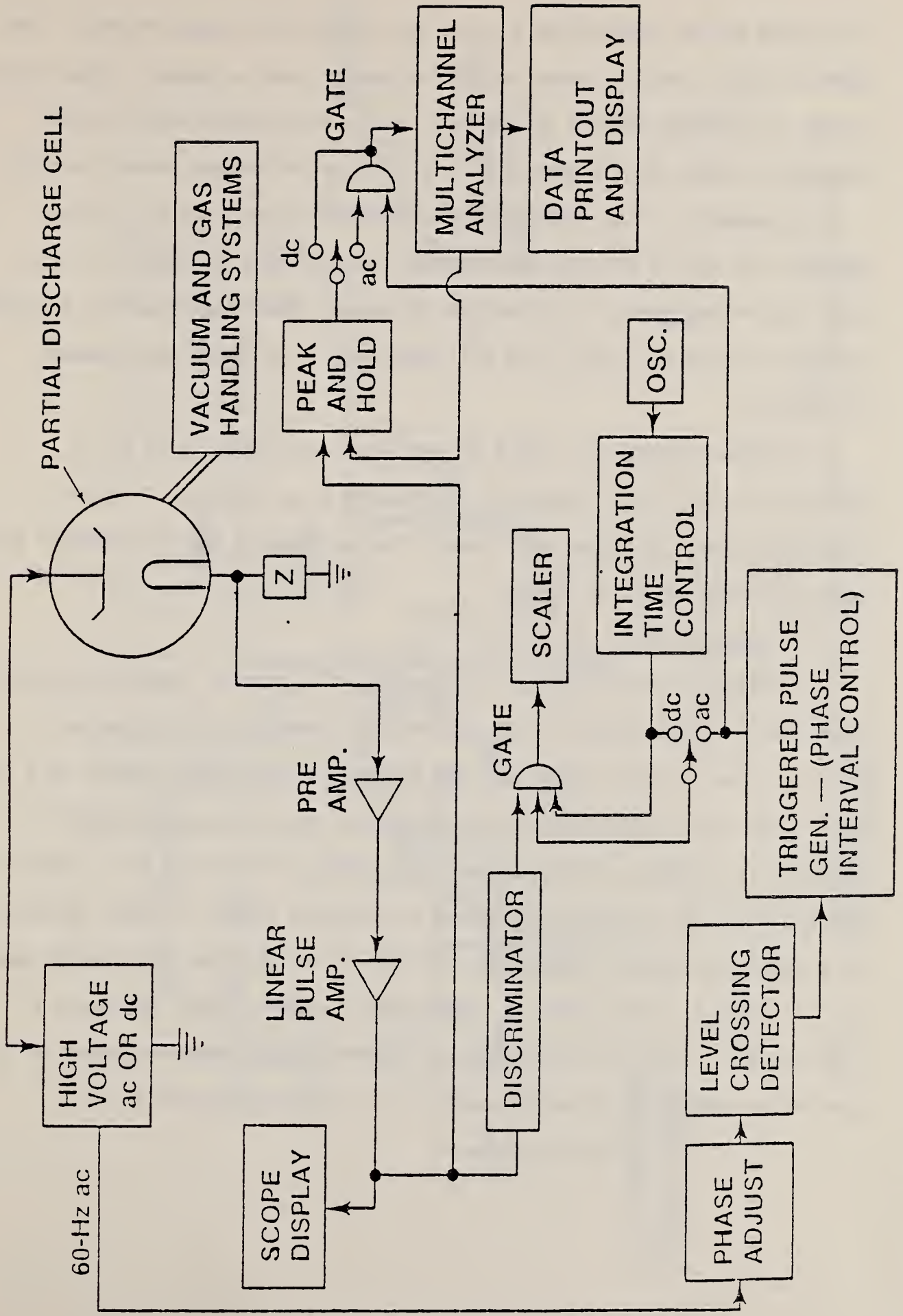

FIG. 1. System used for electrical characterization of 60-Hz ac and dc partial discharges in gaseous dielectrics.

of the MCA can be varied from 5 μs to any arbitrarily large interval. Not shown in Fig. 1 are the electrostatic voltmeter used to measure either the dc or rms ac voltages applied to the cell and an electrometer which can be switched in place of the impedance Z to measure an average corona current.

A schematic of the preamplifier circuit which was used as a corona detector for all of the PHD measurements reported here is shown in Fig. 2. With this arrangement, it is possible to detect individual electron avalanches as small as 0.02 pC (i.e., $\sim 1 \times 10^5$ electrons). For these measurements $Z = 5.0$ kΩ.

The brass corona cell could be evacuated to a pressure of 1.3×10^{-5} Pa ($\sim 1 \times 10^{-7}$ Torr) prior to introducing a gas sample. Polished stainless steel electrodes were used. The gap spacing and tip diameter of the point electrode could be varied.

II.A.3 Data Analysis

An example of the results of a "complete" electrical characterization of positive dc corona in SF_6 at 300 kPa (~3 atm) pressure is illustrated in Fig. 3. Shown in this figure are the measured pulse height spectra on a charge level scale with corresponding current, pulse rate, and pulse shapes as a function of voltage. To place the pulse heights on a charge level scale, it was necessary to calibrate the system by applying pulses of known amplitude V' to a precision variable capacitor (see Fig. 2) which gives an injected charge $q = CV'$ where C is the value of capacitance, usually within the range of 1.0-10.0 pF. The level corresponding to an injected charge q appears at a particular channel n of the MCA where n is roughly proportional to q.

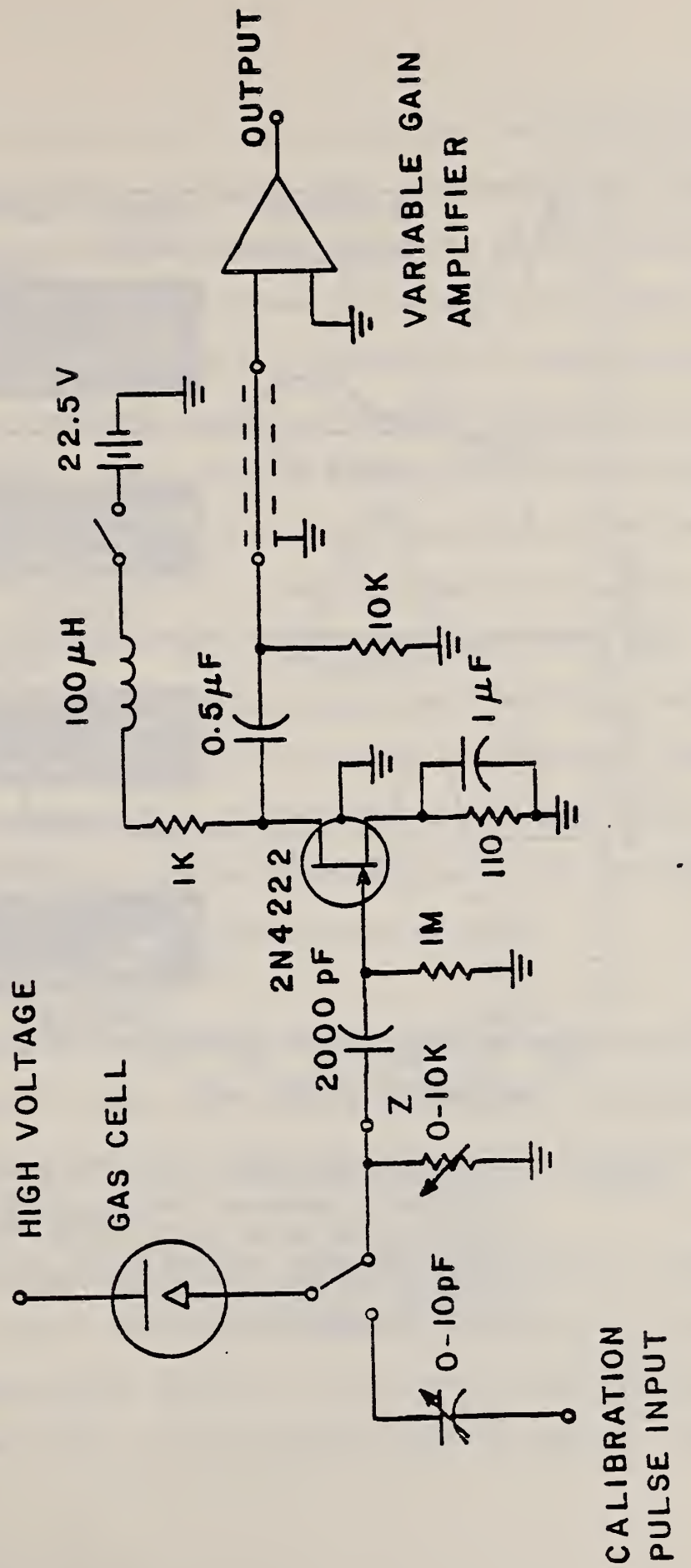

FIGURE 2. Preamplifier circuit used in pulse height distribution measurements as corona detector.

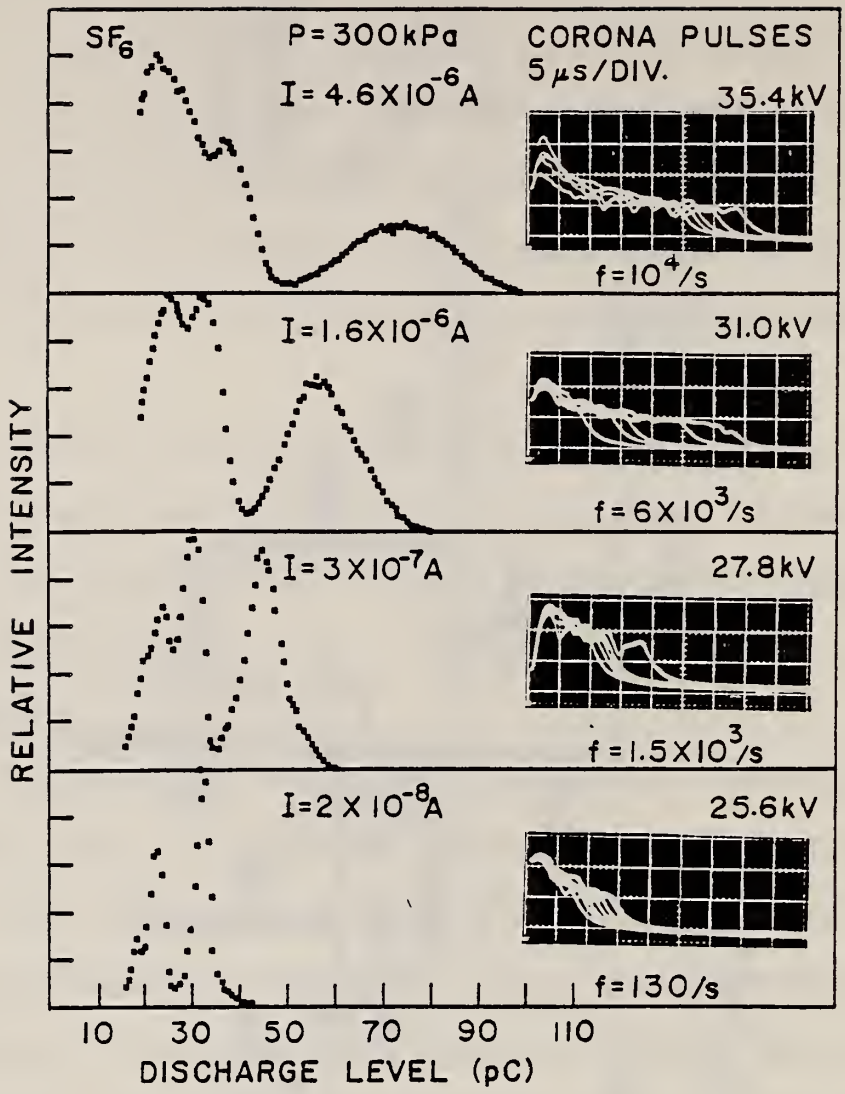

FIGURE 3. Electrical characteristics of positive corona in SF_6 at an absolute pressure of 300 kPa. Shown are the corona pulse shapes, pulse repetition rates, average corona currents and pulse height distributions at the indicated applied dc voltage.

A least-squares straight-line fit to a set of observed points (q_i, n_i), $i \geq 3$ is used to establish the charge level scale from the MCA output. The uncertainty in charge scale calibration depends on charge level and increases as the level decreases. At the present time errors at all charge levels may be as great as 20 percent due in part to uncertainties in matching the time constants of the calibration circuit to the actual corona detection circuit. Further investigations are required to evaluate and reduce this uncertainty.

The PHD data shown in Fig. 3 have been arbitrarily normalized to the maxima in relative intensity. For these data the cut off point at the low charge end is determined by the discriminator level setting used to eliminate noise at the MCA input. The minimum charge level that can be recorded by the MCA is determined by a combination of the gain setting of the variable gain linear pulse amplifier and the discriminator level setting into the MCA. (Note: the discriminator for the MCA is not specifically indicated in Fig. 1, but is an integral part of the peak-and-hold circuit.)

II.A.4 Instrumental Factors

There are several instrumental factors that can have a significant effect on the measurement of PHD's such as the time constant of the detection circuit and the dead time of the MCA. These must be carefully considered lest the results be misinterpreted.

We first consider the effect of MCA dead time (sampling interval). This could be significant if the spacing between pulses such as in a burst is smaller than the sampling interval. If in a burst, the pulses show a regular dependence of amplitude on time during the sampling interval, then the form of

the measured PHD, i.e., the way in which the MCA characterizes the burst, will depend on how much of the burst is actually sampled.

The effect of MCA dead time on the measured PHD is illustrated in Fig. 4 for the case of positive dc corona in SF_6 at a pressure of 200 kPa. The corona in this case occurs predominantly in the form of bursts during which a large primary event is followed by many smaller secondary events; although at this pressure and voltage there are some single, isolated, lower level pulses not associated with bursts. This is illustrated by the oscilloscope trace inset (also see traces in Fig. 3). In Fig. 4, we also show a comparison of PHD data taken under identical conditions with the exception that the MCA dead time is 7 μs in one case and 50 μs in the other. It can be seen that in going from the longer to the shorter dead time there is a major enhancement of the relative contribution of the low charge pulse features. This can be explained by the fact that for the 7 μs time the smaller secondary pulses which occur during burst activity are being sampled, whereas at 50 μs there is little or no contribution from these events since, for the operating conditions chosen, nearly all burst lengths are less than 50 μs.

The 50 μs data, therefore, simply correspond to the PHD for primary initial events of which in this case there appear to be two types as previously noted from the oscilloscope trace of pulses shown. These are namely larger streamer pulses, generally the precursors of bursts, and lower amplitude single avalanche type pulses.[3] These measurements confirm earlier speculation[2] that much of the observed structure in PHD spectra for positive corona in SF_6 is associated with characteristics of pulse bursts, and demonstrates the advantages of using a fast MCA sampling rate for PHD corona characterization.

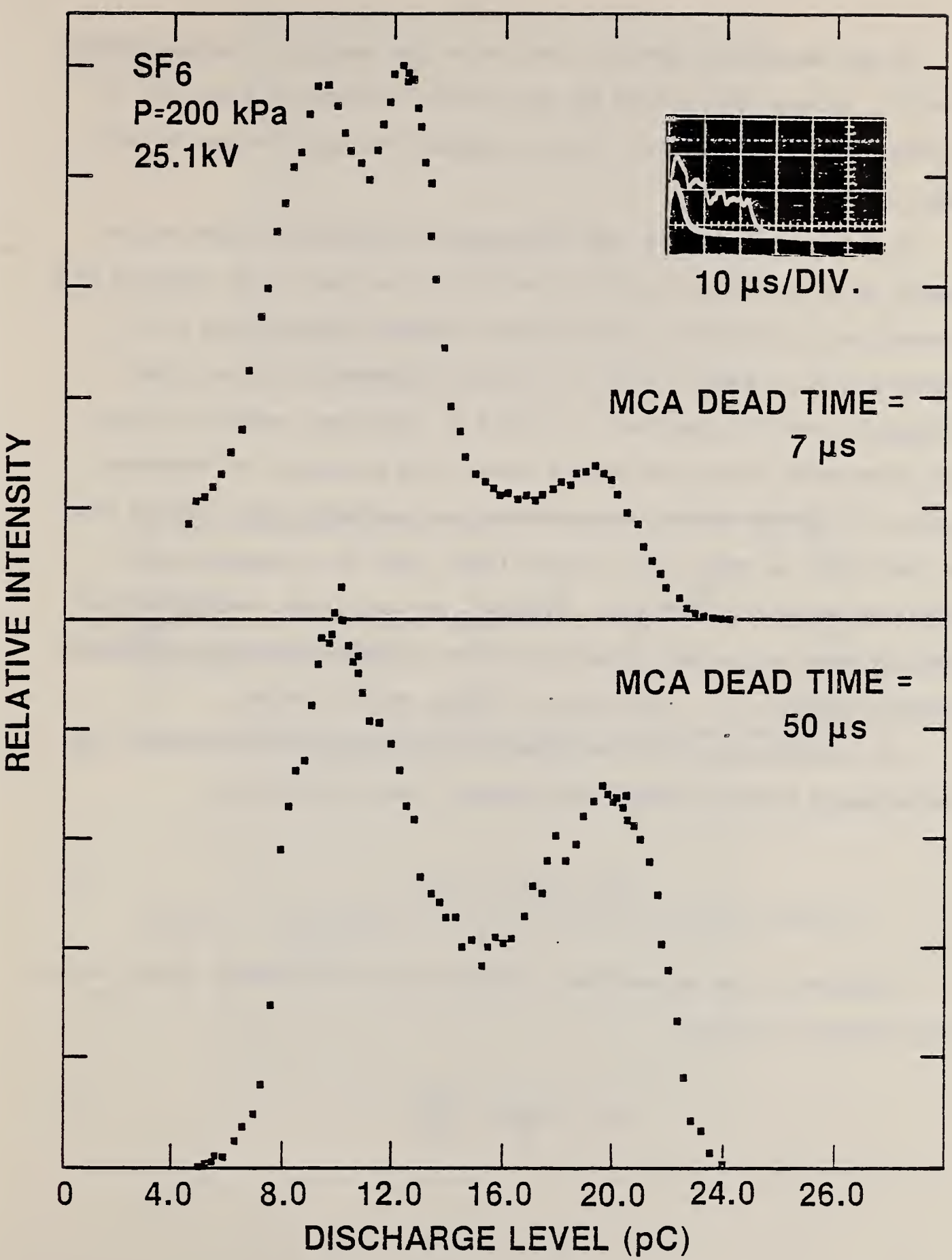

FIGURE 4. Measured partial discharge pulse height distributions in SF_6 for different multichannel analyzer dead times. Also shown in the inset is an oscilloscope trace displaying pulses from three separate partial discharge events, one of which corresponds to a burst.

We next examine the effect of the finite time constant of the measurement circuit. Although this problem has been briefly mentioned (see Ref. 2), it deserves careful consideration. We now consider this question here in more detail.

To a good approximation, the discharge-pulse detection circuit can be modeled as an equivalent circuit consisting of a low pass filter connected to a current source of infinitely high internal impedance corresponding to the discharge cell as shown in Fig. 5. In this arrangement, it is the output voltage V(t) which is measured. It should be recognized, however, that the real measurement circuit may contain several time constants, and therefore consist of a higher order low pass filter than considered here. For the sake of simplicity, we treat only a single filter, since it is expected that a single RC combination dominates. Moreover, the conclusions reached from the analysis below are largely independent of the detailed form of the instrument transfer function, i.e., the effects of higher order filtering.

The instantaneous discharge current i(t) at any time t is related to the instantaneous currents through the capacitor C and resistor R by

$$i(t) = i_C(t) + i_R(t). \tag{1}$$

Equation (1) can be rewritten in terms of the instantaneous charge q(t) on the capacitor C to give

$$i(t) = \frac{q(t)}{RC} + \frac{dq(t)}{dt}. \tag{2}$$

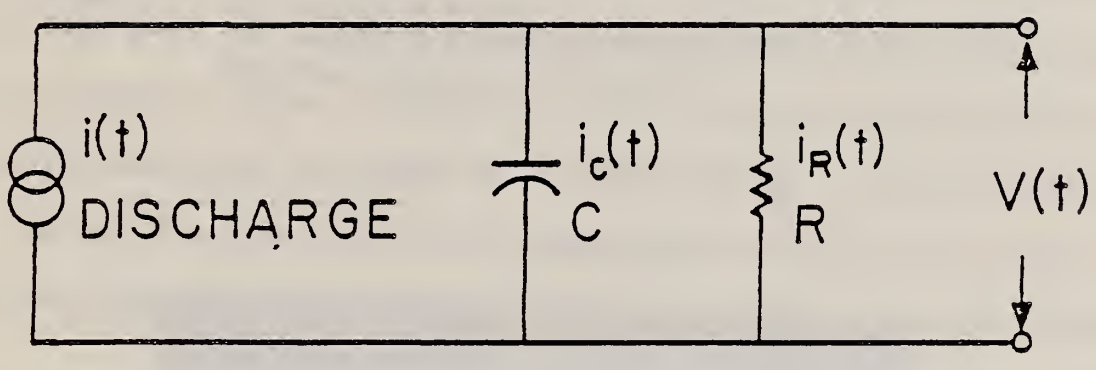

FIGURE 5. Equivalent circuit for partial discharge detection system.

Having solved Eq. (2), the desired output voltage is simply given by

$$V(t) = q(t)/C. \tag{3}$$

Corona pulses, associated with motion of electrons in the electrode gap, are typically of very short duration, i.e., < 10 ns. Fast oscilloscope traces of typical dc corona pulses in our cell with pressurized SF_6 show that they have a duration of less than 4 ns. In Figs. 6 and 7, we show the output display of a fast transient digitizer used to record the shapes of pulses observed when the detector shown in Fig. 2 was replaced by a fast preamplifier for which $Z = 50\ \Omega$. The shapes recorded here are typical of those seen for positive and negative dc corona in SF_6 and indicate a width of about 1 ns or less for these events. Some variation in the shapes of the corona pulses was noted in these high resolution measurements, but this topic will not be discussed further here. More measurements of pulse shape characteristics are underway.

The important point to note here is that the RC time constant of the detection circuit used for PHD measurements (in this case roughly 2.0 μs) is much greater than the corona pulse duration Δt, i.e., $\Delta t << RC$. It should be noted that the choice of RC time constant for this instrument is made on the basis of limitations imposed by the sampling time of 2 μs of the peak-and-hold circuit (see Ref. 16). There is no point in having a detector RC which is much smaller than this.

We now show that if this condition holds ($\Delta t << RC$), then the amplitude of the pulse sampled by the pulse height analyzer is proportional to the area

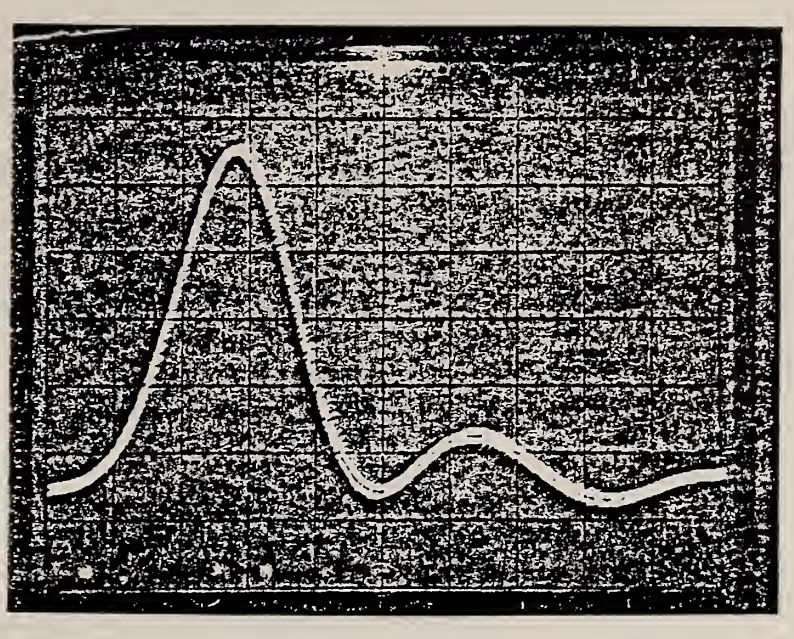

FIGURE 6. Oscilloscope trace of transient digitizer output for a single pulse from positive dc corona in SF_6. The time scale is 0.5 ns/div.

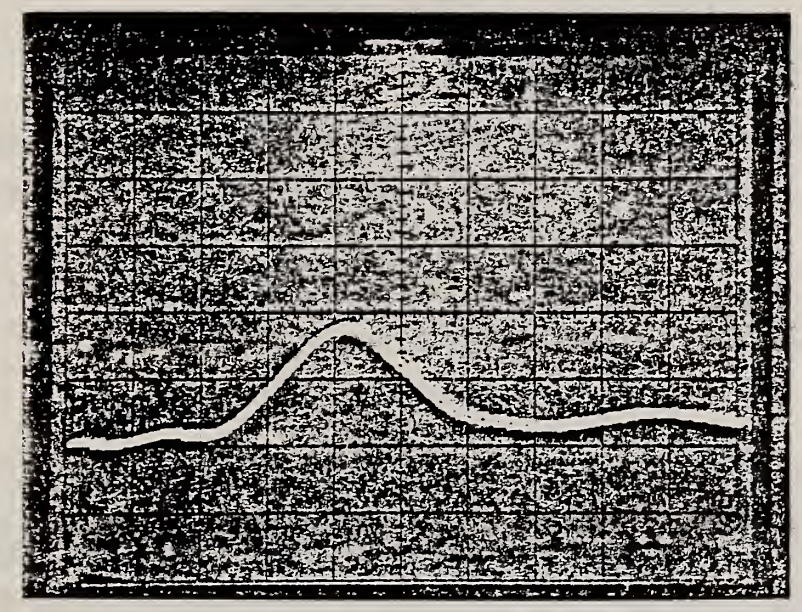

FIGURE 7. Oscilloscope trace of transient digitizer output for a single pulse from negative dc corona in SF_6. The time scale is 1.0 ns/div.

under the corona current and hence directly proportional to the total charge Q in the pulse. To do this we first consider a simplified case where it is assumed that the corona pulse is rectangular and of width Δt, so that $i(t) = i_0$ for $t \leq \Delta t$ and $i(t) = 0$ for $t > \Delta t$; so the net charge in the corona pulse is $i_0 \Delta t$. For $t \leq \Delta t$ the solution of Eq. (2) is

$$q(t) = RCi_0 [1 - \exp(-t/RC)], \tag{4}$$

and for $t > \Delta t$,

$$q(t) = RCi_0 \exp(-t/RC)[\exp(\Delta t/RC)-1], \tag{5}$$

so that the output has a maximum (peak value) at $t = \Delta t$ given by

$$V_{max} = Ri_0 [1 - \exp(-\Delta t/RC)]. \tag{6}$$

If $\Delta t << RC$, then by expanding the exponential we obtain, to a good approximation,

$$V_{max} \cong i_0 \Delta t/C \propto Q. \tag{7}$$

The fractional error of the charge measurement in this case is given mainly by the second term in the expansion and is thus proportional to $(\Delta t/RC)$ which is negligible provided $\Delta t << RC$.

In the more general case of arbitrary i(t) one can calculate the output response using the standard Green's Function approach to solve Eq. (2). The Green's function $G(t,t')$ in this case must satisfy the differential equation

$$\frac{dG(t,t')}{dt'} - \frac{1}{RC} G(t,t') = \delta(t-t') \tag{8}$$

subject to the boundary conditions: $G = 0$ at $t < t'$ and $G \to 0$ as $t-t' \to \infty$. Here $\delta(t - t')$ is the usual Dirac delta function. One can verify that the appropriate function is given by

$$G(t,t') = \begin{cases} 0, & t < t' \\ \exp[-(t-t')/RC], & t > t' \end{cases} . \tag{9}$$

With this function the solution to Eq. (2) is:

$$q(t) = \int_0^{\infty} G(t,t')\, i(t')dt' . \tag{10}$$

At the peak of the output pulse (V_{max}) the condition $dq(t)/dt = 0$ must be satisfied, and this yields the time t_m at which the peak occurs, from which

we have

$$V_{max} = q(t_m)/C. \tag{11}$$

The fractional error ε in determining the charge Q is given by the difference

$$\varepsilon = (Q - q(t))/Q \tag{12}$$

or using Eqs. (9) and (10)

$$\varepsilon = \frac{1}{Q}\left[\int_0^{\infty} i(t')dt' - \int_0^{t_m} i(t')\exp[-(t_m - t')/RC]dt'\right]. \tag{13}$$

Now assuming a relatively short corona pulse so that $i(t) = 0$ for $t > t_m + \delta t$ where $(t_m + \delta t) \ll RC$, we have

$$\varepsilon \simeq \frac{1}{Q}\left[\int_{t_m}^{\delta t + t_m} i(t')dt' + \int_0^{t_m} i(t')\left(\frac{t_m - t'}{RC}\right)dt'\right]. \tag{14}$$

This reveals that the fractional error is proportional to a term on the order of t_m/RC plus an integral over the tail of the corona pulse extending δt beyond t_m. This latter term is also small provided $\delta t \ll t_m$, or if $\delta t \ll RC$. In the simple example considered above, for a symmetric triangular

corona pulse of full width Δt, one can easily show using Eq. (10) and the condition $dq/dt = 0$ that

$$t_m = \Delta t/(1 + \Delta t/RC), \tag{15}$$

and, therefore,

$$\begin{aligned} \delta t &= \Delta t - t_m \\ &= \Delta t[(\Delta t/RC)/(1 + \Delta t/RC)], \end{aligned} \tag{16}$$

from which it is seen that indeed $\delta t \simeq 0$ provided $\Delta t/RC << 1$.

There are, of course, cases where one cannot assume $\delta t << t_m$ such as are known to occur for some Trichel pulses that have an extended tail associated with ion conduction following the initial electron charge transport across the gap.[17] A phenomenon, similar to Trichel pulses, which exhibits this behavior has been observed in our laboratory for negative corona in SF_6 at pressures less than 60 kPa, and at voltages close to onset. In Fig. 8, we show an oscilloscope trace of these negative corona pulses and the corresponding PHD. They are like Trichel pulses observed in other electronegative gases in that they occur with nearly constant amplitude and exhibit a long tail which can extend more than 100 μs beyond the initial pulse. Unlike true Trichel pulses, however, the spacing between them is random. The PHD profile is that expected from sharp pulses of nearly constant amplitude followed by a long tail. The high background level on the low charge side of the main peak in the PHD is not due to small pulses, but rather results from the sampling several

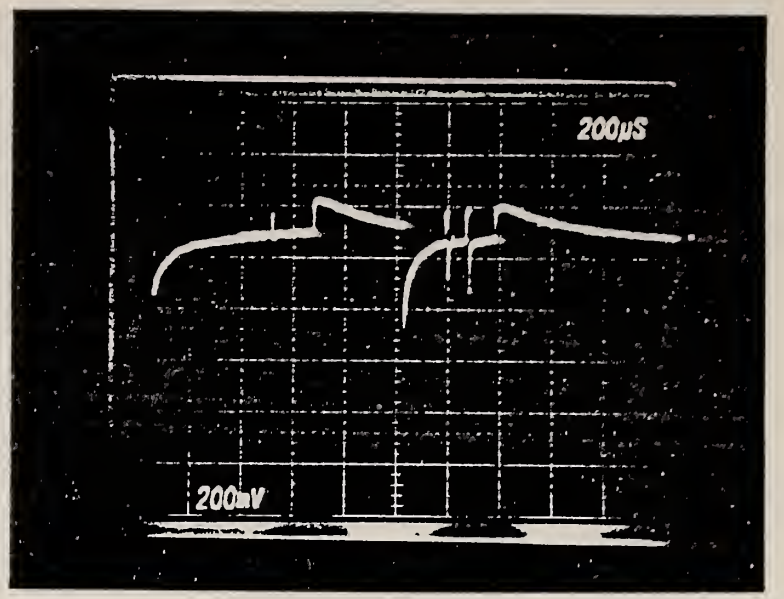

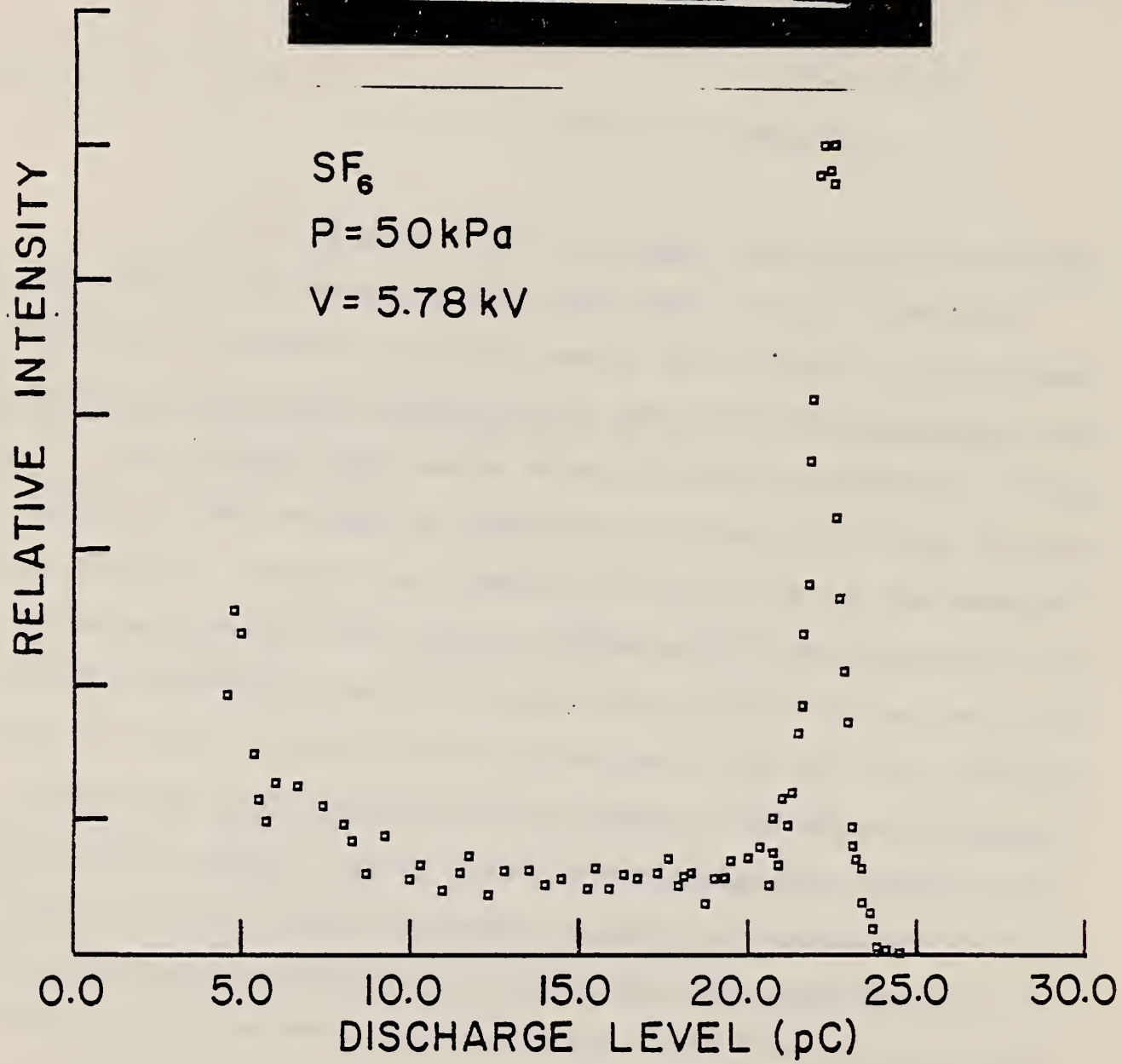

FIGURE 8. Pulse shapes and corresponding pulse height distribution for negative "Trichel like" corona pulses in SF_6 at an absolute pressure of 50 kPa. The corona was generated at a voltage of 5.78 kV using a point plane electrode geometry with a point diameter of 0.08 mm and gap spacing of 1.24 cm.

times the long tail which necessarily decays with a time constant characteristic of the measurement circuit. The positive upswing in the oscilloscope trace corresponds to the point where the current associated with the long tail abruptly extinguishes. It is clear, in this case, that the condition $\delta t << t_m$ is not satisfied and the charge level at the PHD peak near 22.4 pC does not include the charge in the tail associated with ion transport across the gap.

In the case of pulse bursts such as have been observed for positive dc corona in SF_6, there are complications in the interpretation of PHD measurements (in addition to those noted previously) that depend on the multichannel analyzer dead-time. The added complications arise if the spacing between burst pulses t_c is less than the RC time constant of the measurement circuit. This is certainly the case for our observation of positive corona pulses in SF_6 at pressures above about 100 kPa. In Fig. 9 are shown oscilloscope traces of positive corona pulse bursts observed with a detection circuit having a time constant of 0.1 μs which is to be compared with our usual PHD measurement circuit with a time constant of ∿2.0 μs as noted above. There seem to be two relatively distinct regions of the burst following an initial streamer event. Immediately after the initial event a group of pulses appears with a spacing of ∿0.1 μs, then a later group appears with a larger spacing of 0.5 μs. The spacing in either case is less than, or at most comparable to, the RC time constant of the circuit.

In examining the problem that occurs here, we consider two extreme cases, namely when $t_c >> RC$ and when $t_c << RC$. In the first case, one is obviously measuring the charge of single pulses in the burst, i.e., the PHD

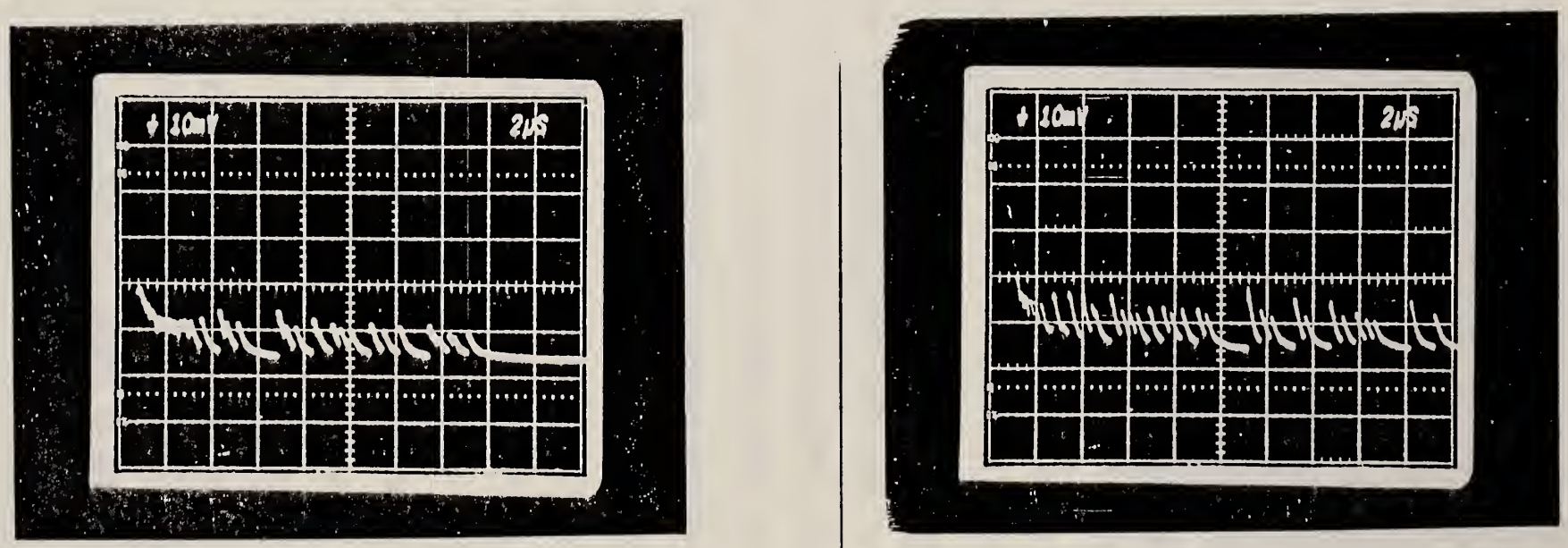

FIGURE 9. Positive corona pulse bursts in SF_6 at 300 kPa observed with circuit having a 0.1 μs time constant. The time scale of both traces is 2.0 μs/division.

corresponds to isolated corona events. For the other extreme, this is not the case, and it can be shown that what one is measuring here is the sum of the charges included in the burst pulses sampled. To demonstrate this, we consider the simple example of two rectangular pulses of the same amplitude i_o and width Δt such that the spacing t_c between them satisfies the condition $\Delta t + t_c << RC$. The solution to Eq. (2) gives a maximum of

$$q(t_m) = RC\ i_o\ [1-\exp(-\Delta t/RC)]\ [1 + \exp[(-t_c-\Delta t)/RC]] \tag{17}$$

which for $t_c + \Delta t << RC$ reduces to

$$q(t_m) = i_o(2\Delta t), \tag{18}$$

i.e., the sum of the charges in the two pulses. In reality, the situation is intermediate between these extreme cases, and the measured amplitude for a burst in which $t_c < RC$ will be in general greater than that associated with charge in a single pulse, but less than the net charge in all pulses included in the sampling interval.

We have considered in the above discussion some of the fundamental limitations of the PHD measurement technique which should be understood if one is to properly interpret results. In particular, because of the necessity of using a detection circuit with a finite time constant and because of the finite sampling rate of the multichannel analyzer, one is not always measuring the true pulse height or charge distribution spectrum of partial discharges. The result of the measurement is rather a convolution of the instrument impulse

response function with the input signal from the discharge as is the case with any measurement system. Nevertheless, the PHD measurement is a useful method for statistically quantifying the characteristics of corona in a reproducible way and, as will be shown later, is a sensitive indicator of gas contamination, electrode surface conditions, and changes in these induced by the corona. This technique should be further studied with the goal of optimizing the information content of the data so that it can be readily correlated with data from other diagnostic measurements.

II.A.5 Results and Conclusions

The results of many measurements of the electrical characteristics of dc corona pulses in SF_6 and SF_6/N_2 mixtures have already been summarized in Ref. 2. In particular, a report is given there of the voltage and pressure dependence of corona pulse height distribution and pulse repetition rates measured using the apparatus described here. In addition to the data given in Ref. 2, measurements have recently been made to check the dependence of SF_6 corona characteristics on gap spacing and on irradiation of the gap with uv light from an Hg-discharge lamp. The previously reported PHD data[2] were obtained using a point-plane electrode gap of 1.24 cm. Measurements were also made for a 2.28 cm gap. In this case, the partial discharge PHD's for positive and negative corona exhibited features quite similar to those seen with the smaller gap, i.e., the essential PHD characteristics remain unchanged as the gap is increased.

The effect of irradiating the gap with uv light was also investigated for positive SF_6 corona. Particular attention was given to cases, to be noted later, where relatively large effects of radiation on pulse repetition rates

were observed. It has thus far been discovered that, even in cases where radiation causes an order of magnitude or more increase in repetition rate, the PHD characteristics remain virtually unchanged.

The results presented in Ref. 2 will not be reproduced here, but the general conclusions are worth repeating. The conclusions drawn from this work pertain to point-plane positive and negative dc corona in SF_6 at pressures in the range of 50 to 500 kPa. For positive corona the conclusions are listed below.

1) Positive corona starts as low level avalanches which rapidly develop into streamer pulses or pulse bursts that increase in mean amplitude and repetition rate as the applied voltage is increased. Typical pulse amplitudes are in the range of 10 - 100 pC.

2) The burst length of positive corona pulses decreases and the mean amplitude increases with increasing gas pressure.

3) Positive corona PHD's broaden and pulse burst lengths increase with increasing applied voltage.

These conclusions are consistent with other observations of positive dc corona in SF_6.[10,11] It has been proposed[10] that the burst characteristics of the corona, such as burst length and mean spacing of pulses in the burst, are controlled by the development of space charge in the inter-electrode gap. The initial event of largest amplitude corresponds to an

electron avalanche or streamer which propagates into a gap free of space charge. The negative ion space charge which this event creates moves towards the point, locally enhancing the electric field and producing, via detachment, avalanche-initiating electrons which give rise to secondary events in the burst. These secondary avalanche events cannot propagate as far into the gap due to the shielding effect of the residual positive ion space charge, and thus will necessarily be of lower amplitude than the primary event. Once the level of positive space charge builds up to some critical point the burst will extinguish. One sees then that the duration of the burst will be controlled by the rate at which the positive ion space charge builds up which, in turn, is governed by the rate at which positive ions move toward the plane. At higher pressures (or lower applied voltages) the positive ions will move more slowly, thus positive ion space charge will build up more rapidly and consequently the pulse bursts will diminish in length. In this way, one can, at least qualitatively, understand the observed pressure and voltage dependence of positive dc corona burst characteristics in SF_6.

The conclusions for negative dc corona in SF_6 are listed below.

1) The predominant mode of negative corona in SF_6 is a quasi-glow consisting primarily of many small (<3 pC) closely spaced pulses, although there is a tendency as pressure decreases below 400 kPa for negative corona to begin as somewhat larger pulses $\sim$10 pC, see Fig. 8.

2) The pulse repetition rate for negative corona in the quasi-glow mode is usually an order of magnitude greater than for positive corona at comparable average current.

There is evidence from measurements made using SF_6/N_2 mixtures that the corona characteristics, particularly the PHD's, are quite sensitive to small changes in gas composition. Further investigation of this is underway, and more will be said about this later.

II.B. Comparison of AC and DC Corona Inceptions in SF_6

II.B.1 Motivation

There has been some concern about the extent to which data on dc corona inceptions can be used to predict what will happen under 60-Hz ac conditions. The argument is often heard that 60 Hz is slow enough compared to the duration of a typical corona event that it is essentially like dc. There exists reason to believe however that even at gas pressures slightly above 100 kPa ($\sim$1 atm) the development of ion space charge in a gap can be quite different under ac and dc conditions so that differences in corona phenomena should be evident. The extent to which this is true has not previously been clear. Again this work has been motivated by the general lack of useful fundamental data on SF_6 corona. There also exists the problem of defining inception voltage in such a way that a meaningful comparison can be made between ac and dc conditions. We have performed measurements, discussed below, which help examine this question. Preliminary results of this study have already been reported (see Ref. 1).

II.B.2 Apparatus and Measurement Technique

The apparatus used to generate and detect corona in SF_6 is the same as that previously described in Sec. II.A. (see Fig. 1). For both ac and dc voltages the onset of corona was determined by observing and recording individual corona pulses. Because SF_6 corona in the pressure range 50 to 500 kPa appears initially in the form of pulses, it was deemed that pulse

detection would be the most satisfactory way of making comparative inception measurements (preferable, for example, to a measurement of current). For the ac measurement, a gating circuit arrangement (see Fig. 1) was employed so that corona pulses could be observed only during predetermined phase intervals of the 60-Hz sine wave. In this way it was possible to separate positive and negative inceptions for ac.

The voltages applied to the electrodes were measured for both ac and dc conditions with the same electrostatic voltmeter. In the case of ac, this meter gives the rms value. Thus it was necessary to calculate peak values assuming a pure sine wave. The ac voltage values reported here for onset are the calculated peak values.

Measurements were made both with and without irradiation of the gap with light from an Hg-discharge lamp through a quartz window. Inception was defined, in all cases, as the intercept of a straight line fit to the data on a semi-log scale with the voltage axis determined by the 0.1 count/s level. For these measurements, the level of sensitivity for corona pulse detection was in the range of 0.05 to 0.02 pC.

Applying the same definition of inception to both ac and dc conditions leads to some difficulties in making a meaningful comparison. One could reason, assuming identical instantaneous field conditions, that near onset, the measured discharge repetition rate for 60 Hz should be reduced relative to that for dc by roughly the fraction $\Delta t/T$ where Δt is the time interval in the sine wave during which the voltage exceeds the threshold value and $T = 0.0167$ s corresponding to the period for 60 Hz. One would thus expect, given the definition for inception chosen here, that the onset for 60 Hz should be

somewhat higher than for dc. This is indeed observed to be the case as will be seen later when comparison is made between ac and dc negative corona inceptions where, because these both occur for gaps presumed initially free of space charge, instantaneous onset field conditions are the same. However, for sharply rising onsets such as occur for negative corona in SF_6, the error associated with neglecting the factor $\Delta t/T$ in comparing ac to dc is relatively small.

II.B.3 Results

Examples of data on corona pulse repetition rate versus voltage are shown in Figs. 10 - 14. The data shown are for positive and negative dc corona in SF_6 at different gas pressures both with and without uv irradiation of the gap. The open symbols correspond to data obtained with radiation, and the different symbols correspond to measurements made at different times. The data in Figs. 10 - 12 were obtained with a point-to-plane gap spacing of 1.24 cm whereas the data in Figs. 13 - 14 correspond to a gap of 2.28 cm. The point electrode tip diameter was 0.09 mm for both cases. The measurements were performed using polished stainless-steel electrodes. At each pressure, a fresh SF_6 gas sample was used after the cell had been evacuated. It is apparent, from the data shown here, that positive corona in SF_6 initially develops at a much slower rate than negative corona, and the curve of repetition rate versus voltage exhibits a sudden increase in slope several kilovolts above threshold. This increase in slope appears to be associated with the development of the pulse burst activity as evident from corresponding pulse height distribution measurements (see previous section).

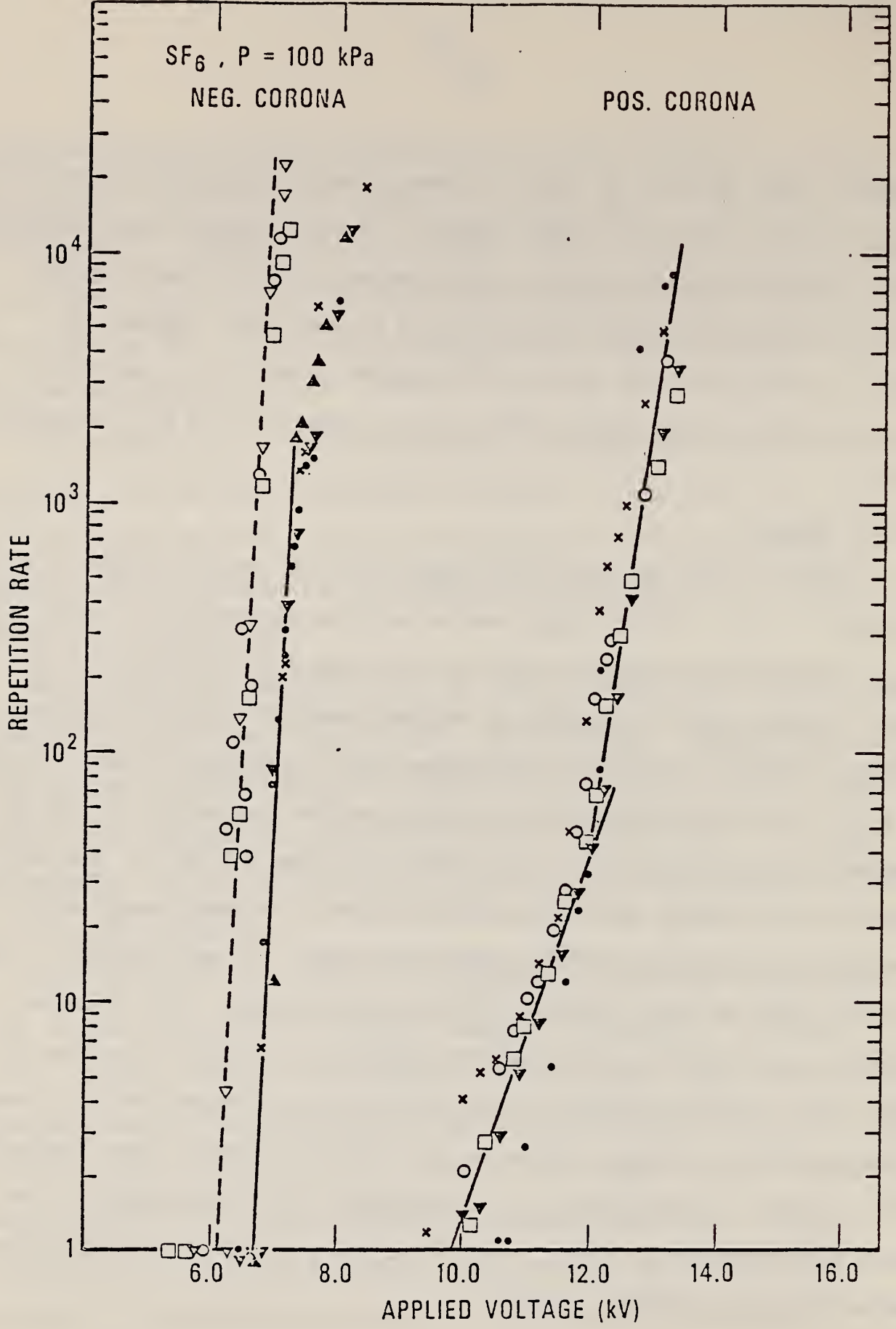

FIGURE 10. Partial discharge repetition rate versus applied voltage for positive and negative, point-plane dc corona in SF_6 at an absolute pressure of 100 kPa. The open symbols correspond to measurements made with an irradiated gap.

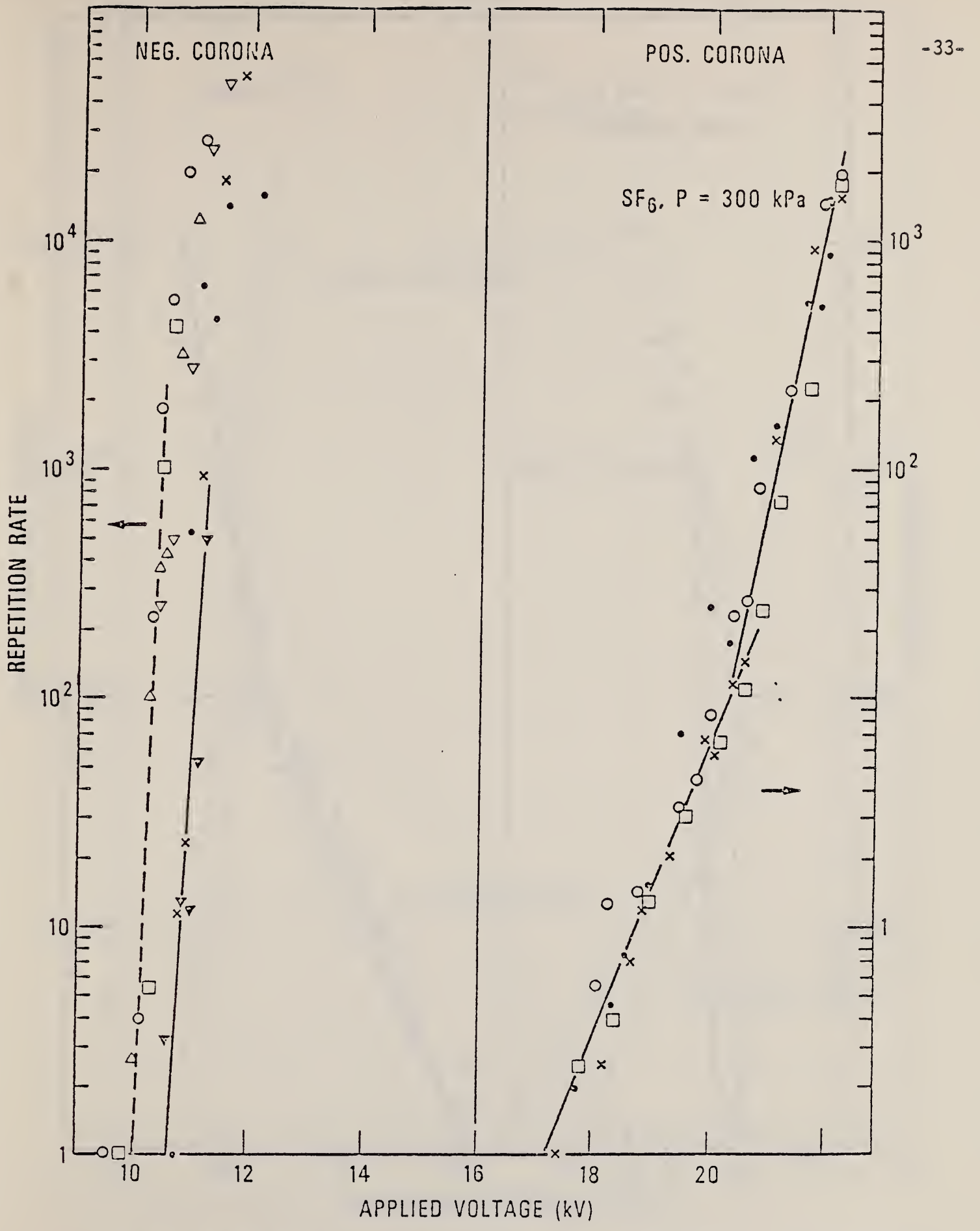

FIGURE 11. Partial discharge repetition rate versus applied voltage for positive and negative, point-plane dc corona in SF_6 at an absolute pressure of 300 kPa. The open symbols correspond to measurements made with an irradiated gap.

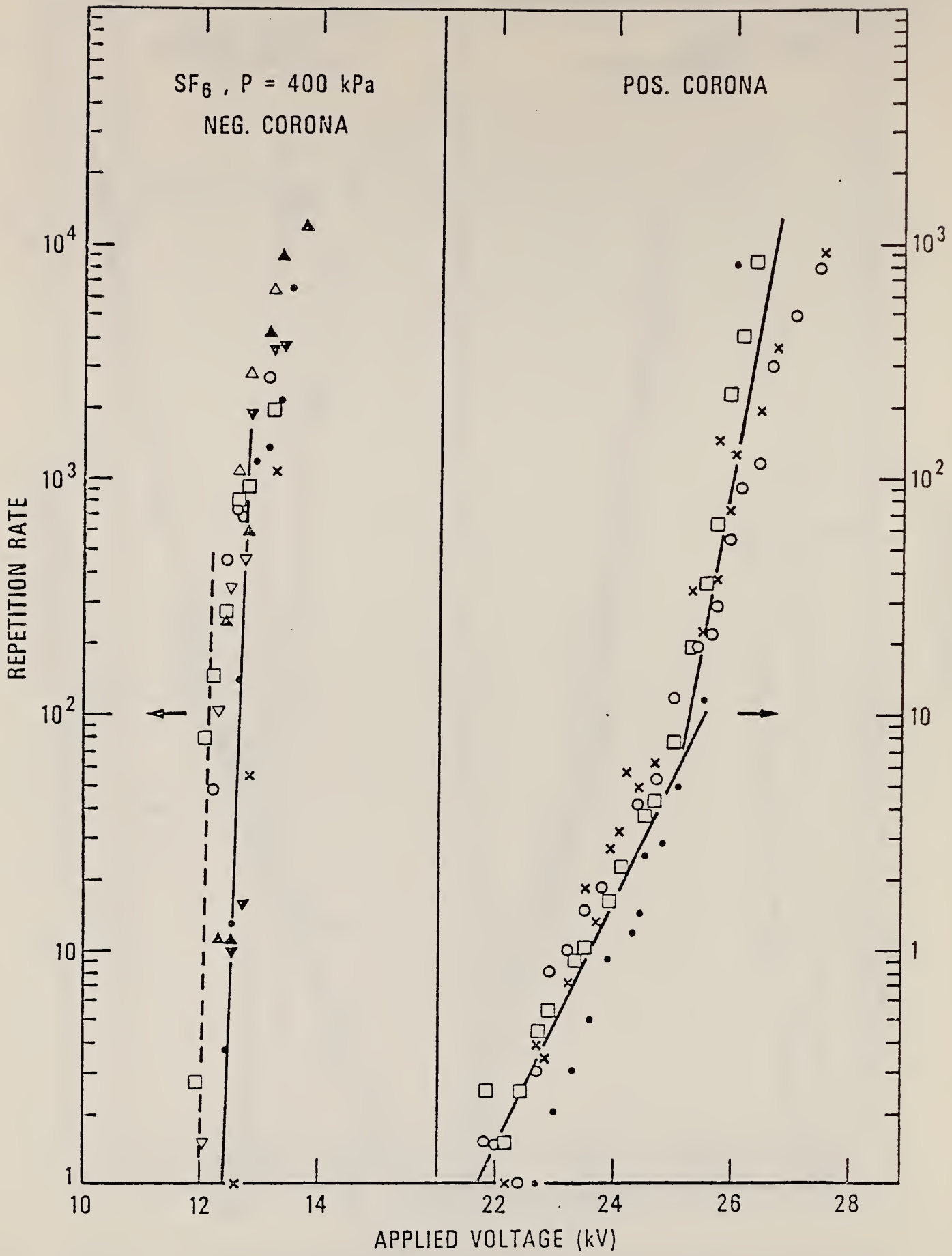

FIGURE 12. Partial discharge repetition rate versus applied voltage for positive and negative, point-plane dc corona in SF_6 at an absolute pressure of 400 kPa. The open symbols correspond to measurements made with an irradiated gap.

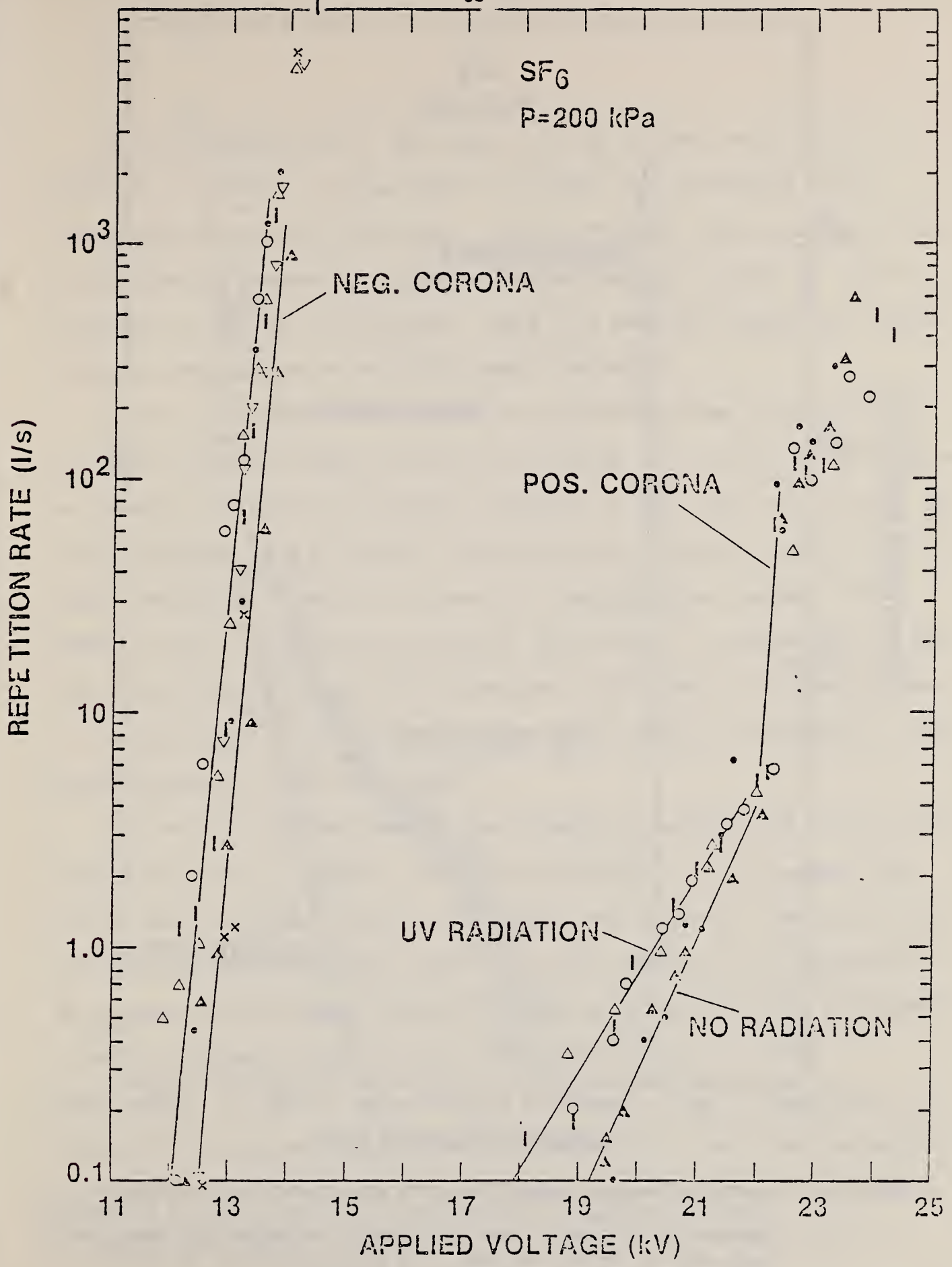

FIGURE 13. Partial discharge repetition rate versus applied voltage for positive and negative, point-plane dc corona in SF_6 at an absolute pressure of 200 kPa. The open symbols correspond to measurements made with an irradiated gap. The point-plane gap spacing is 2.28 cm and the point diameter is 0.09 mm.

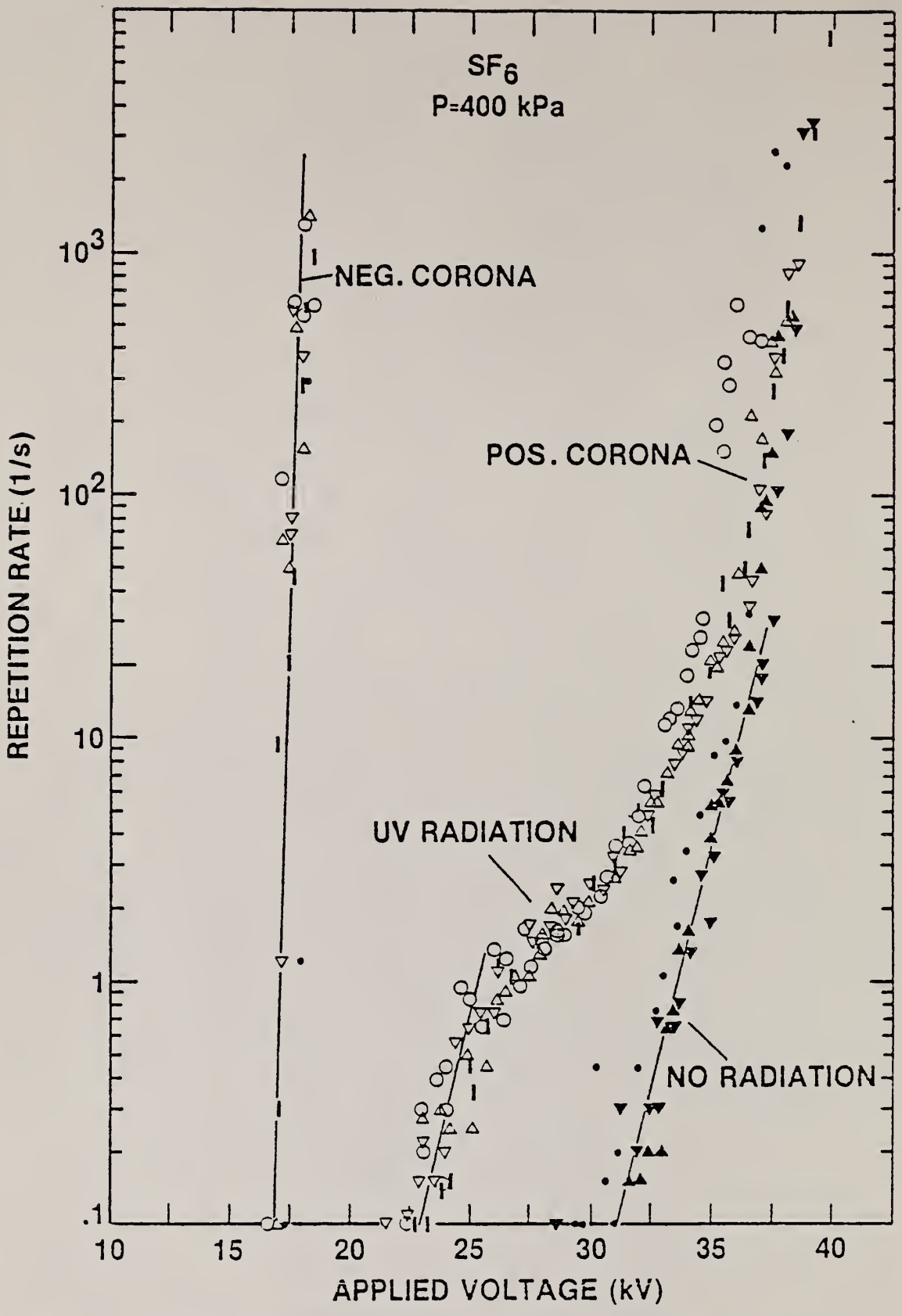

FIGURE 14. Partial discharge repetition rate versus applied voltage for positive and negative point-plane dc corona in SF_6 at an absolute pressure of 400 kPa. The open symbols correspond to measurements made with an irradiated gap. The point-plane gap spacing is 2.28 cm and the point diameter is 0.09 mm.

For SF_6 gas pressures in the range of 100 to 500 kPa, the effect of uv radiation on negative dc corona onset is slightly more pronounced for the 1.24 cm gap than for the 2.28 cm gap. As seen from the figures, however, even in this case the presence of radiation reduces the onset voltage by less than 10 percent of that for no radiation. There is a tendency, though, for results to become somewhat more reproducible under irradiation.

For the 1.24 cm gap, the presence of uv radiation seems to have little or no effect on the development of positive dc corona. In the case of the 2.28 cm gap, however, the effect of radiation inception is seen from Figs. 13-14 to be quite pronounced. The difference between positive inceptions measured with and without radiation is found to increase with increasing gas pressure. The effect is clearly greatest near inception where corona is predominantly in the form of low level avalanches and progressively diminishes as voltage increases to the point where self-sustaining streamer bursts develop corresponding to an abrupt increase in repetition rate.

For the 60-Hz ac measurements, the presence of radiation has little or no observable effect on inception at either gap spacing. One could argue that this is expected because, under ac conditions near threshold, the fraction of time that the voltage exceeds threshold is small compared to 100 percent for the dc case and, therefore, the radiation may not cause observable enhancement in partial discharge count rate for light intensities used in these measurements. For the ac case, there is simply not as much time available for photons to initiate avalanches. Also as noted earlier, near onset the measured discharge repetition rate for 60 Hz should be reduced relative to that for dc by roughly the fraction $\Delta t/T$. Since this fraction might be quite small it

would be difficult to observe changes in pulse repetition rates close to threshold where the already low (0.1 to 1 count/s) pulse rates for dc must be reduced by $\Delta t/T$.

The results of determining inception values from data such as shown in Figs. 10 - 14 are summarized in Figs. 15 and 16 which show positive and negative ac and dc inception voltages as a function of SF_6 gas pressure for the two point-plane gap spacings.

II.B.4 Discussion

An understanding of the physical basis for the rather large effect (see Figs. 14 and 16) of irradiation on the development of electron avalanches at positive dc corona inception in SF_6 would be desirable. At this point one can only speculate. One plausible explanation is that the uv enhances initiating-electron production in an active volume near the point via photodetachment of negative ions. Table I shows the predominant Hg emission lines from the lamp used with their corresponding energies and relative intensities. The table also shows electron affinities of various negative ions that might be present in the gas. Although the available photon energy is not sufficient to photoionize SF_6, it is sufficient to photodetach negative ions likely to be present. As gas pressure is increased, one might expect formation of negative ion clusters of the type $(SF_6^-)(SF_6)_n$ where $n \geq 1$ (see Refs. 18 and 19). Unfortunately the electron affinities of these species are not known, but detachment from these are likely to be at least as probable as from simpler molecular negative ions; also their mobilities are expected to be lower enabling them to remain longer in the active volume where free electrons,

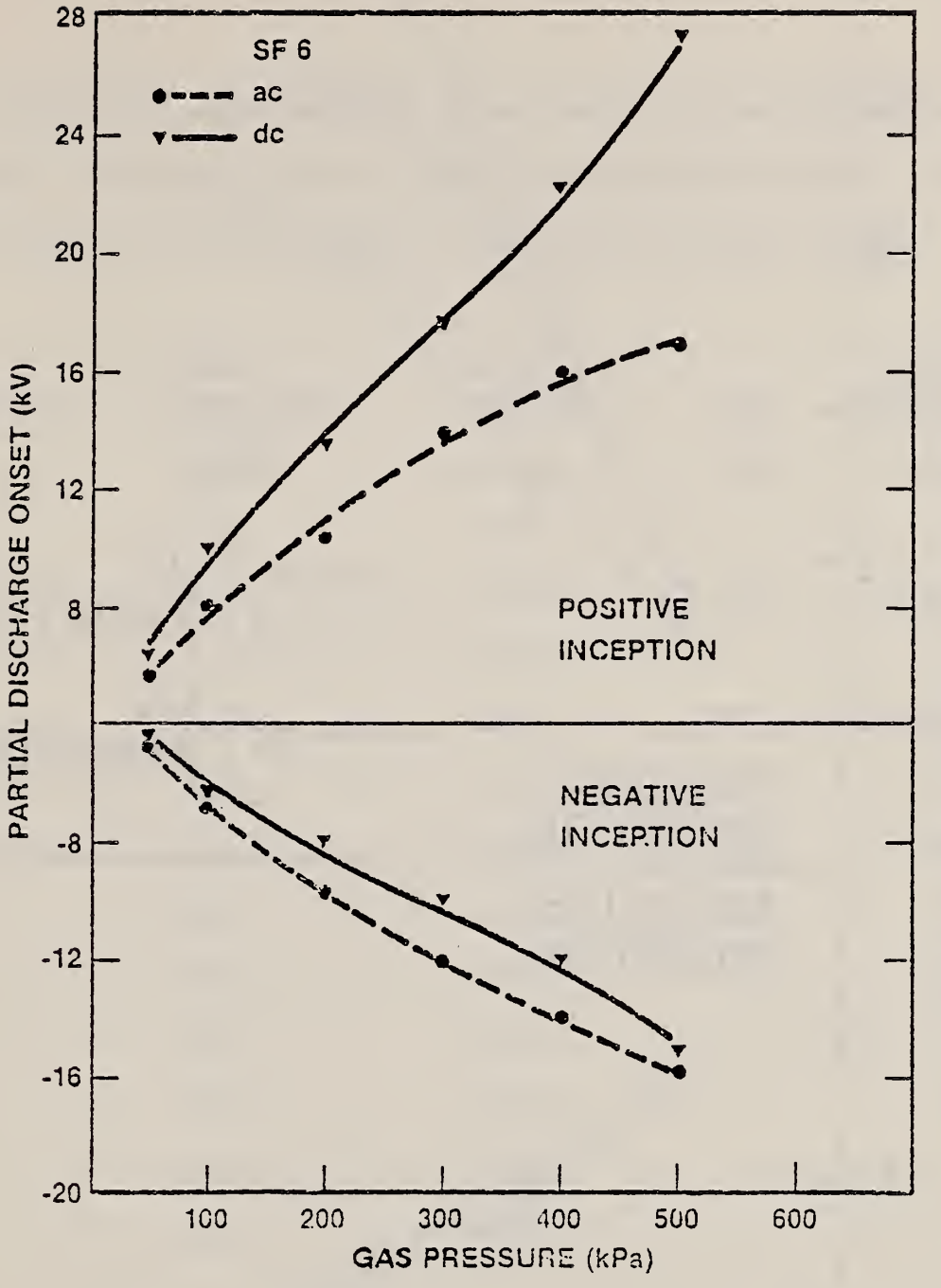

FIGURE 15. Comparison of ac and dc positive and negative corona inceptions for SF_6. The measurements were performed at room temperature using stainless steel point-plane electrodes with a gap spacing of 1.24 cm and a point diameter of 0.09 mm. The gap was irradiated with uv light from a mercury discharge lamp.

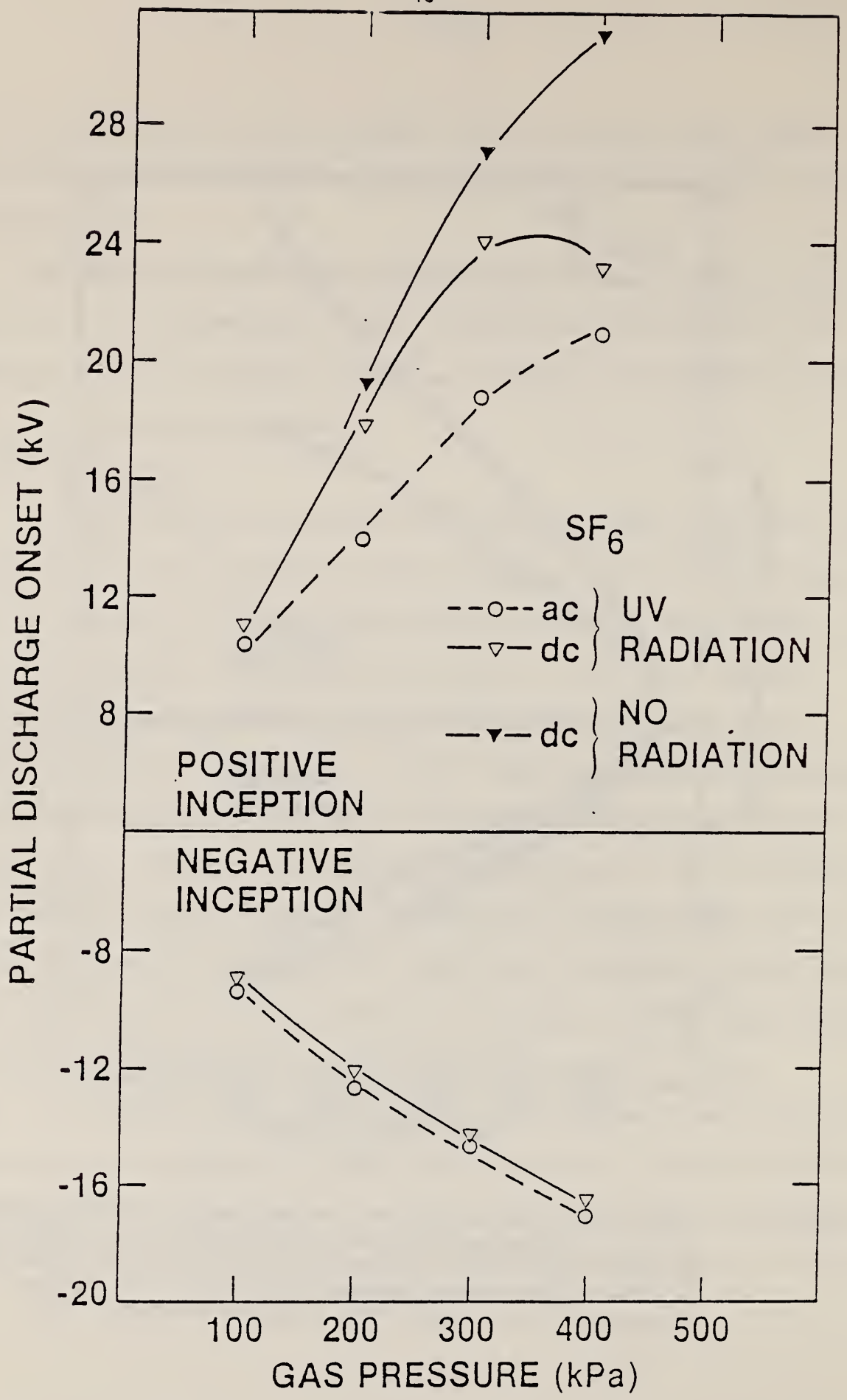

FIGURE 16. Comparison of ac and dc positive and negative corona inceptions for SF_6. The measurements were performed at room temperature using stainless steel point-plane electrodes with a gap spacing of 2.28 cm and a point diameter of 0.09 mm. The open points correspond to data taken with the gap irradiated by a mercury discharge lamp.

Table I: Predominant atomic emission lines from Hg discharge lamp used for gap irradiation indicating relative photon intensities and energies, and electron affinities of various negative ions possibly present in SF_6.

Photon Wavelength (nm)	Photon Energy (eV)	Relative Intensity	Ion	Electron Affinity
295	5.46	0.419	SF_6^-	0.6eV
305	4.13	0.562		
325	3.8	0.351	SF_5^-	2.7eV
355	3.49	0.654		
365	3.40	1.00	F^-	3.4eV
395	3.14	0.357		
405	3.07	0.442	SO_2^-	1.1eV
425	2.92	0.525		
435	2.85	0.622	O^-	1.5eV
535	2.32	0.422		
545	2.28	0.659		
565	2.20	0.339		
575	2.16	0.641		

released by detachment, can initiate avalanches thus explaining pressure effects.

The photon intensity and wavelength dependence of avalanche formation probability in an irradiated gap should be checked. Preliminary measurements indicate that the avalanche formation rate increases with light intensity. However, it has not yet been determined that there is, for example, a saturation effect which might be expected once the intensity is high enough to photodetach all of the ions in the active volume where free electrons can lead to avalanche formation. Wavelength dependence measurements might give an indication of the negative ions involved if photodetachment is indeed the initiation mechanism. By checking dependence of avalanche production on light beam position, one might also learn about the extent of the active region where avalanches originate.

Referring to Figs. 15 and 16, it can be seen that under all conditions the ac and dc negative inceptions appear at lower absolute values than the positive inceptions. Also there is reasonable agreement between the ac and dc negative inceptions, the small difference probably being accounted for by the assumed definition for onset as discussed above. The polarity effect seen here has previously been noted [11,20] for dc point-plane corona in SF_6. At the present time, however, there exists no theoretical prediction of the magnitude of this effect. One could speculate that this effect is physically reasonable because the corona-initiating electrons for a negative point are necessarily generated in the high field region near the point as opposed to the lower field region away from the point where positive corona originates. Thus negative corona might be expected to appear at lower voltages. On the other hand, the

polarity difference may also be due in part to different roles that the point electrode surfaces play in initiation of positive and negative corona. The reasons for this effect thus remain open to question.

It is also seen in Figs. 15 and 16 that, in the case of positive corona, the dc inceptions are always higher than the corresponding ac inceptions, and there is a tendency, at least for results obtained without irradiation, for this difference to increase with increasing gas pressure. This difference, we believe, can be attributed to the effect of ionization from corona in the negative half cycle influencing development of corona on the subsequent positive half cycle.

To determine if this explanation is plausible, we have estimated the time required for various negative ions formed in corona to clear the gap before polarity reversal has occurred. Negative ions that do not reach the positive plane electrode before polarity reversal can be attracted back to the point electrode, locally enhancing the field and thus lowering the inception voltage. The velocity v of a negative ion moving across the gap on the x-axis, defined by a line from the point electrode perpendicular to the plane, is

$$v(x,t) = \frac{dx}{dt} = k\ E(x)\ \cos\ \omega t, \tag{19}$$

where k is the ion mobility (drift velocity per unit field) assumed independent of field and E(x) is the magnitude of the x-component of electric field. This equation can be integrated to yield a limiting mobility value k_ℓ, below which

no ion at a distance ℓ from the plane would reach the electrode in a quarter cycle, i.e.,

$$k_\ell = \frac{2\pi}{T} \int_0^\ell dx/E(x), \tag{20}$$

where T is the period of the 60-Hz field.

To calculate the electric field between the point-plane electrodes, space charge in the gap was neglected and the electrode system was conveniently approximated as a hyperboloid of revolution over a plane. The static field is described then by the expression[21]

$$E_\eta = \Phi_o \left[f \sin \eta(\cosh^2\xi - \cos^2\eta)^{\frac{1}{2}} \tanh^{-1} (\cos \eta_o)\right]^{-1}, \tag{21}$$

where η and ξ are meridian coordinates in a prolate spheroidal coordinate system, f is half the focal distance, and Φ_o is the potential of the point. A tracing of an enlarged photograph of the point electrode permitted its characterization as a surface of constant η (η_o). For the special case of an ion trajectory along the electrode axis ($\xi = 0$) we obtain, using Eqs. (19) and (21) and $x = f \cosh \xi \cos \eta$,

$$\sin^3 \eta d\eta = k\Phi_o \cos \omega t \, dt \left[f^2 \tanh^{-1} (\cos \eta_o)\right]^{-1}, \tag{22}$$

which, when integrated, replaces Eq. (20) to give k_ℓ.

The mobilities of negative ions produced in SF_6 discharges have been measured.[18,19] The mobility values given by Patterson[19] for the ions SF_6^-, SF_5^-, $SF_6^-(SF_6)$ and $SF_6^-(SF_6)_2$ have been adjusted for pressure P assuming a P^{-1} dependence, and are indicated in Fig. 17. Schmidt et al.,[18] concluded that their data indicate a P^{-1} dependence below ∿100 kPa, but a $P^{-1.25}$ dependence above this pressure suggesting different physical processes occur as pressure increases. Mobility values of Schmidt et al., are also shown in Fig. 17 and compared with k_ℓ values calculated for two ion trajectories corresponding to $\xi=0$ and $\xi=0.5$.

Regardless of the choice of mobility data, it can be seen from Fig. 17 that negative ions produced in SF_6 may not clear the gap before polarity reversal and can thus lead to a space-charge-enhanced field on the positive half cycle. As pressure is increased, more of the negative ions are expected to survive the period of polarity reversal, thereby increasing the possible buildup of space charge. This can explain the increase with pressure of differences between ac and dc positive corona inception voltages. Calculations are presently being made to check the model proposed here. These involve examination of electric field enhancement near the positive point electrode which would result from a negative-ion space charge cloud of reasonable charge density. The objective is to determine if the field can be sufficiently enhanced by space charge in the gap to account for the corona inception differences observed.

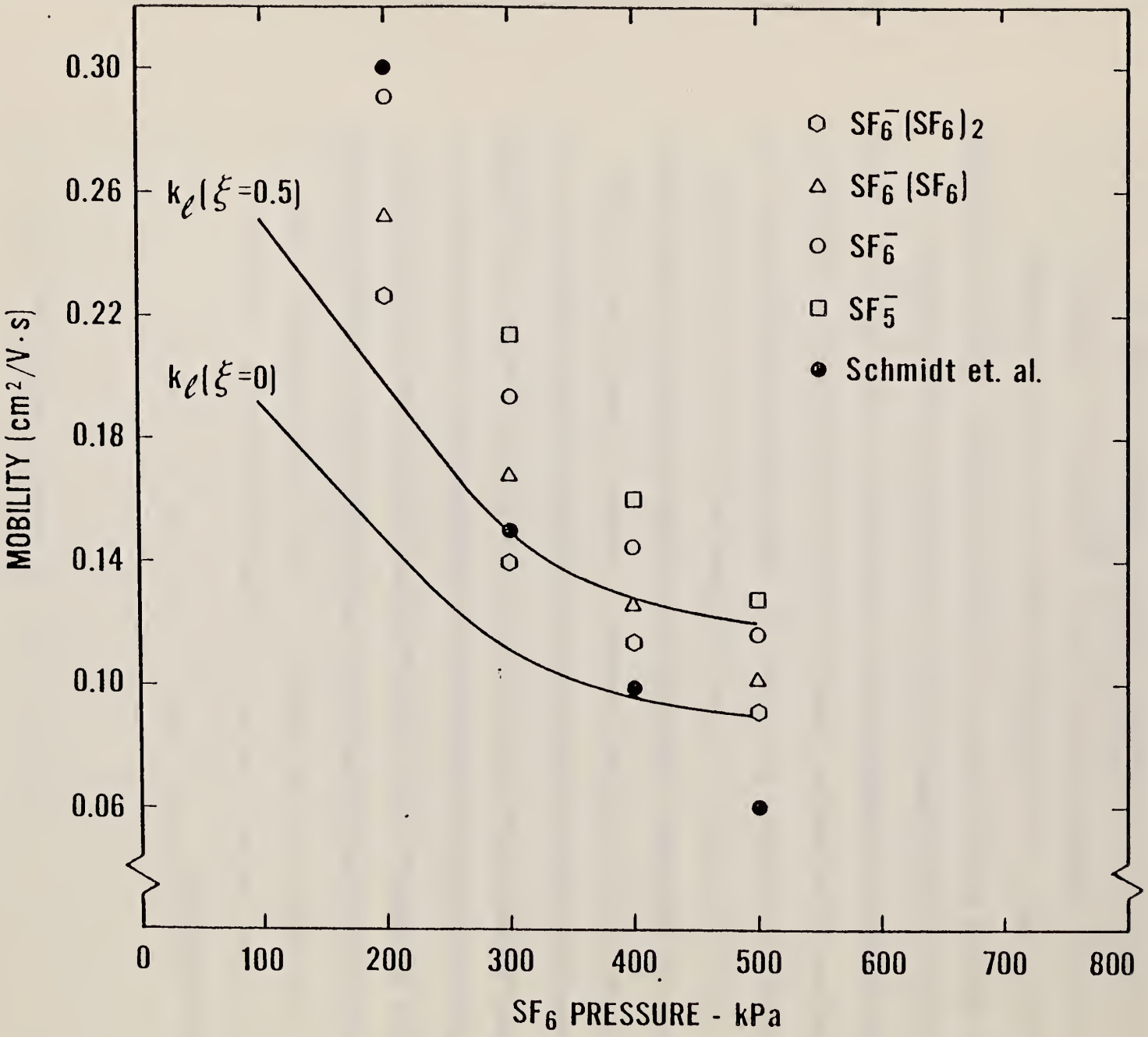

FIGURE 17. Limiting values of ion mobility, k_ℓ along the two ion trajectories given by $\xi=0$ and $\xi=0.5$ as a function of SF_6 pressure. Negative ions produced in SF_6 and tranversing the two trajectories must have mobilities smaller than those indicated by the corresponding curves in order to survive the time to polarity reversal. The open data points are experimental results of Patterson (Ref. 19) extrapolated to pressures above 100 kPa assuming an inverse dependence. The closed data points represent values of negative ion mobilities measured at pressures above 100 kPa by Schmidt, et al (Ref. 18).

II.C. Identification of Corona Induced Decomposition Products in SF_6

II.C.1 Motivation

Although there have been numerous studies of decomposition in SF_6 produced by high power discharges, arcs, circuit breaker operation, etc.[22-28], very little has been done to look at decomposition in low level corona discharges which do not significantly heat the surrounding gas.[29] Decomposition in corona is more difficult to study because it occurs more slowly, and even after hours of operating the discharge, the products may only appear at trace levels. Thus sensitive analytical techniques must be employed. On the other hand, the rate of decomposition can be controlled more readily than in an arc by controlling the discharge power level. A controlled corona discharge may prove to be a superior way of evaluating relative stability of gaseous dielectrics under conditions of excessive electrical stress. Also one should not infer from arc data what can happen for corona, since the nature of these discharge processes are quite different.

Again the importance of understanding how gaseous dielectrics degrade in partial discharges is reemphasized. Corona occurs, in practical systems, around conducting particles, surface protrusions, and at interfaces, and is known to cause insulation deterioration. As metal-clad gas insulated systems are designed to operate at higher and higher stresses, it may be more difficult to avoid corona. The long term stability of an insulating system can be seriously affected by the occurrence of corona if even on an intermittent basis. There are practical situations where corona cannot be avoided, and, in fact, for some applications, such as in the insulation of high energy particle

accelerators, corona is deliberately generated in the insulating gas to insure uniform field distributions.

In our studies reported here, we have chosen to use a gas chromatograph-mass spectrometer (GC/MS) system to perform chemical analysis of the gas which has been subjected to continuous corona generated by applying dc voltage to a point-plane electrode system. This method has its limitations in as much as highly reactive species like HF, or species that easily hydrolyze such as SF_4, require very specialized, complicated gas handling and sampling techniques in order to be observed with any reasonable degree of sensitivity. In general, however, the GC/MS is one of the most sensitive analytical instruments available and can be used to detect most species of interest. In this work, we have identified the decomposition products generated in pressurized SF_6 for point-plane corona operated under conditions of both constant voltage and constant current for many hours.

II.C.2 Apparatus and Measurement Technique

Chemical analysis of SF_6 gas degraded by corona was performed with a modified commercially-available GC/MS system equipped with a data processor. The gas chromatography process can be briefly described as follows. A steady stream of inert "carrier gas," usually helium, is made to flow through a tubular "column" designed so that its surface is encountered frequently by each gas molecule in the stream. The column may be a fine capillary or a wider tube packed with one of a great variety of porous materials known as column supports. The mixture of gases or vapors to be analyzed is introduced near the entrance of the column and is swept into it by the carrier gas stream.

Molecules of different species progress along the column at different rates, because the molecules repeatedly get retained by adsorption on the surface (or in solution, if the column has a liquid coat) for different lengths of time, owing to their different degrees of affinity for the stationary solid or liquid of the column. Different molecules of the same species progress at nearly the same rate, despite some inevitable variation due to nonuniformities of the column and to diffusion. Passage through the column, therefore, separates a gas mixture, causing each component of the original mixture to emerge, or to "elute," from the column at a different time. A detector at the column exit, which in the present case is a mass spectrometer, measures the arrival rate of material other than carrier gas, and the time record from this detector is the chromatogram, showing "abundance" versus "retention time." A column will be unable to separate some components of a mixture if they are too similar in their chemical behavior toward the materials used in that column. Which kind of column to use, under what conditions of temperature and flow rate, is a matter of judicious choice, and the lore of chromatography is vast.

For most of the results reported here, the column in the GC consisted of Porapak Q[30] (80/100 mesh) in 3.2 mm diameter Teflon[30] tubing which was 90 cm in length. For most of the measurements, the column was operated at 24°C with He carrier gas flow rate of about 32 mL/min. Some measurements were performed using a longer glass column with the same support material. In this case, retention times were longer but the same species were observed with roughly the same degrees of sensitivity as for the column mentioned above.

For the column conditions noted above, the absolute pressure at the injection port was 250 kPa. The gas samples to be analyzed (both in

calibration and corona experiments) were extracted from a vessel using a gas-tight sampling syringe. In the usual sampling procedure, for SF_6 at 300 kPa for example, the volume of the sampling syringe was expanded to 1.33 times its original size to give an estimated resulting gas pressure in the syringe of 225 kPa. This was slightly less than the pressure at the injection port; thus, when the syringe was connected to the injection port and unlocked (valve opened), gas did not flow into the chromatograph until the plunger of the syringe was pushed. At the time that the syringe was unlocked, a small amount of carrier gas flowed into the syringe, but this did not affect the measurements. Under the conditions mentioned above, the retention time for SF_6 was 0.5 minutes from the time of injection.

The gaseous species eluting from the column were detected with the mass spectrometer. A membrane separator was used between the GC and MS. The mass spectrometer, in order to separate electrically molecules of different masses, must first ionize the molecules, by bombarding them with 70-eV electrons. These not only ionize the molecules but dissociate many of them as well, in a characteristic pattern. The ion fragmentation pattern, i.e., mass spectrum, serves as a unique signature for identification of the species. Abundant standard reference mass spectral data are available to allow identification of nearly all gaseous species of interest. The data processor for the system, in fact, contains a library of standard mass spectra which can be used for immediate, on-line comparison with measured spectra. The mass spectra of all decomposition species reported here have been verified.

Once the mass spectra of the decomposition products had been identified, it was advantageous to operate the system in the single-ion monitoring mode.

In this procedure, the mass spectrometer is set to look only at selected ion species of a given mass-to-charge ratio (m/e), namely those ions most abundant in the mass spectra of the products to be detected. By this mode of operation, one can achieve higher detection sensitivity--down to the ppm by pressure level.

For some of the important decomposition products, namely the oxyfluorides SOF_2 and SO_2F_2, as well as SO_2, an attempt was made to calibrate the GC/MS so that quantitative analysis of gas concentration could be performed. Because of difficulties in preparing reliable standard gas samples of known concentration, we have thus far been unable to calibrate the system for the important species H_2O, HF and SF_4. In the case of the latter two species, no serious attempt has yet been made to detect these species. They could be detected only with extreme difficulty and much reduction in sensitivity with the GC column conditions described here.

In performing the calibration, checks were made on the proportionality of the GC/MS response to the concentrations of SOF_2 and SO_2F_2 in SF_6. Using 0.4 mL samples of 500 ppm, 250 ppm, 125 ppm, 63 ppm, 31 ppm, 16 ppm, and 8 ppm of SOF_2 in SF_6, we found the response ratio $[SOF_2(m/e=67)/SF_6(m/e=70)]$ to be equal to the known sample concentration ratio times 102 ±1 (one standard deviation), where it is suspected, however, that the observed agreement is somewhat fortuitous. The single-ion chromatograms for m/e=86, corresponding to these measurements, are shown in Fig. 18. With 1.0 mL samples and larger uncertainties, $[SOF_2/SF_6]$ could be measured down to the 1 ppm level.

For SO_2F_2, using 0.4 mL samples of concentrations of 500 ppm, 250 ppm, 125 ppm, and 63 ppm, we found the response ratio

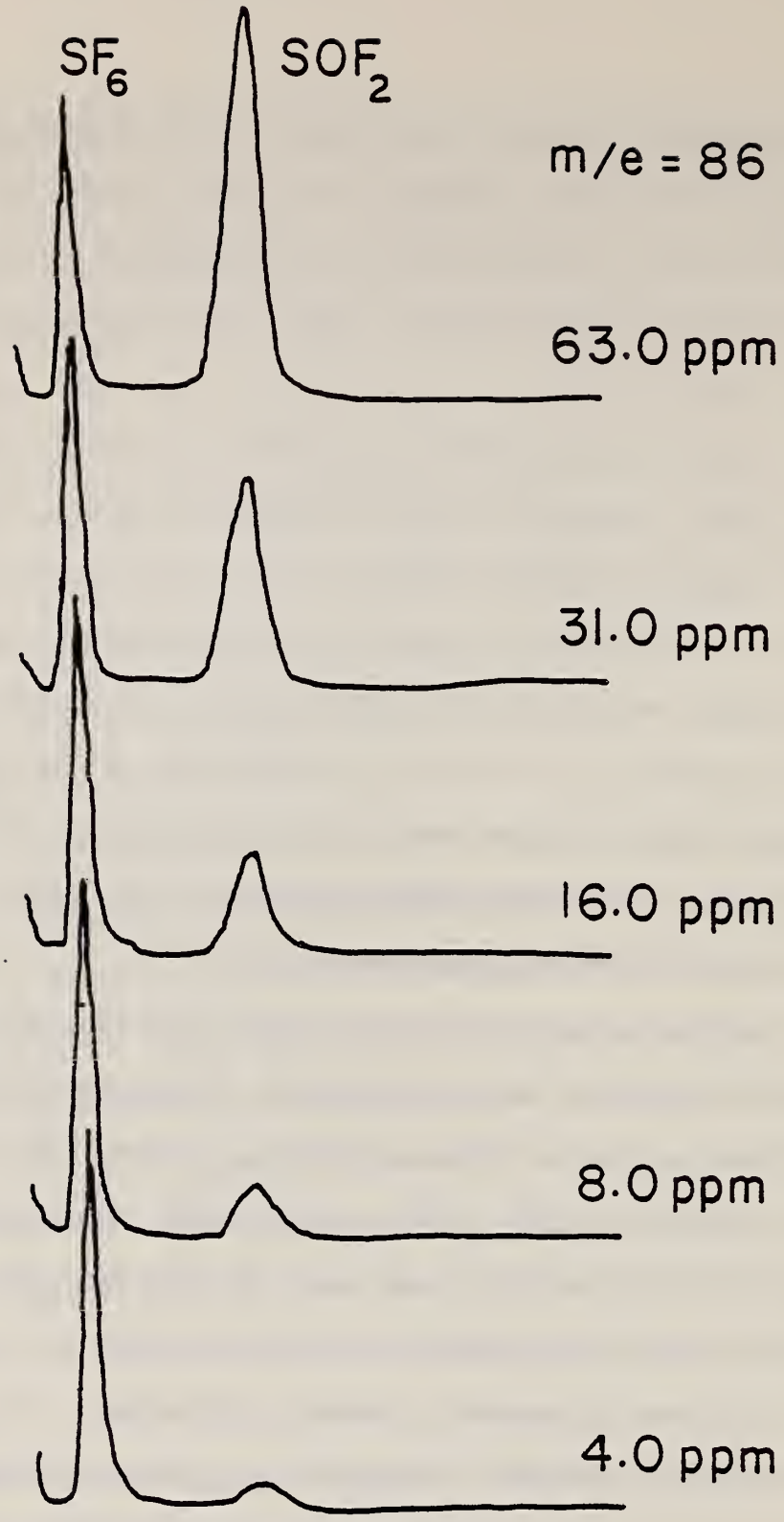

FIGURE 18. Single ion chromatograms for ion of mass-to-charge ratio of 86 from gas samples containing the indicated concentrations of SOF_2 in SF_6. Shown are the SOF_2^+ peaks and an ion feature from SF_6 as a function of retention time.

[SO_2F_2(m/e=102)/SF_6(m/e=70)] to be equal to the concentration ratio times 59 ±3 (one standard deviation). Again, with 1.0 mL samples, SO_2F_2/SF_6 could be measured down to 1 ppm, but the uncertainties were large. The chief difficulty with some of our measurements of SO_2F_2 is that the signal associated with ions from this species appears just after the SF_6 response which, because it is so much more intense, perturbs the baseline in an unpredictable way. This problem is illustrated by the single ion chromatograms shown in Fig. 19 for the ion SO_2F^+ from SO_2F_2 with m/e=83. In this case, the SO_2F^+ peak is preceded by a dip in signal level which we believe is due to a momentary reduction in the ion multiplier gain resulting from the intense bombardment of ions from SF_6. Recently, our measurements of SO_2F_2 have been more accurate due to the discovery of GC column conditions which allowed greater separation between the SO_2F_2 and SF_6 features.

In preparing the standard samples for calibration, a large syringe was used to extract the trace constituent of interest from a lecture bottle containing pure gas which was then injected into a 4.0 liter volume into which the desired quantity of pure SF_6 was later introduced. For SOF_2 and SO_2F_2, we injected 4.0 mL of both gases at 150 kPa into the 4.0 liter cell, and then filled the cell with SF_6 to a pressure of 300 kPa. In this way, we obtained a well-mixed 500 ppm mixture of SOF_2 and SO_2F_2 in SF_6.

After analyzing this mixture, we made it twice as dilute by doubling the SF_6 pressure allowing the gas to mix for a few minutes, then pumping half of it away (until the pressure was 300 kPa as before). This procedure of analysis and dilution was repeated until the SOF_2 and SO_2F_2 concentrations constituted only 1.0 ppm of the mixture. Although we have no proof that the

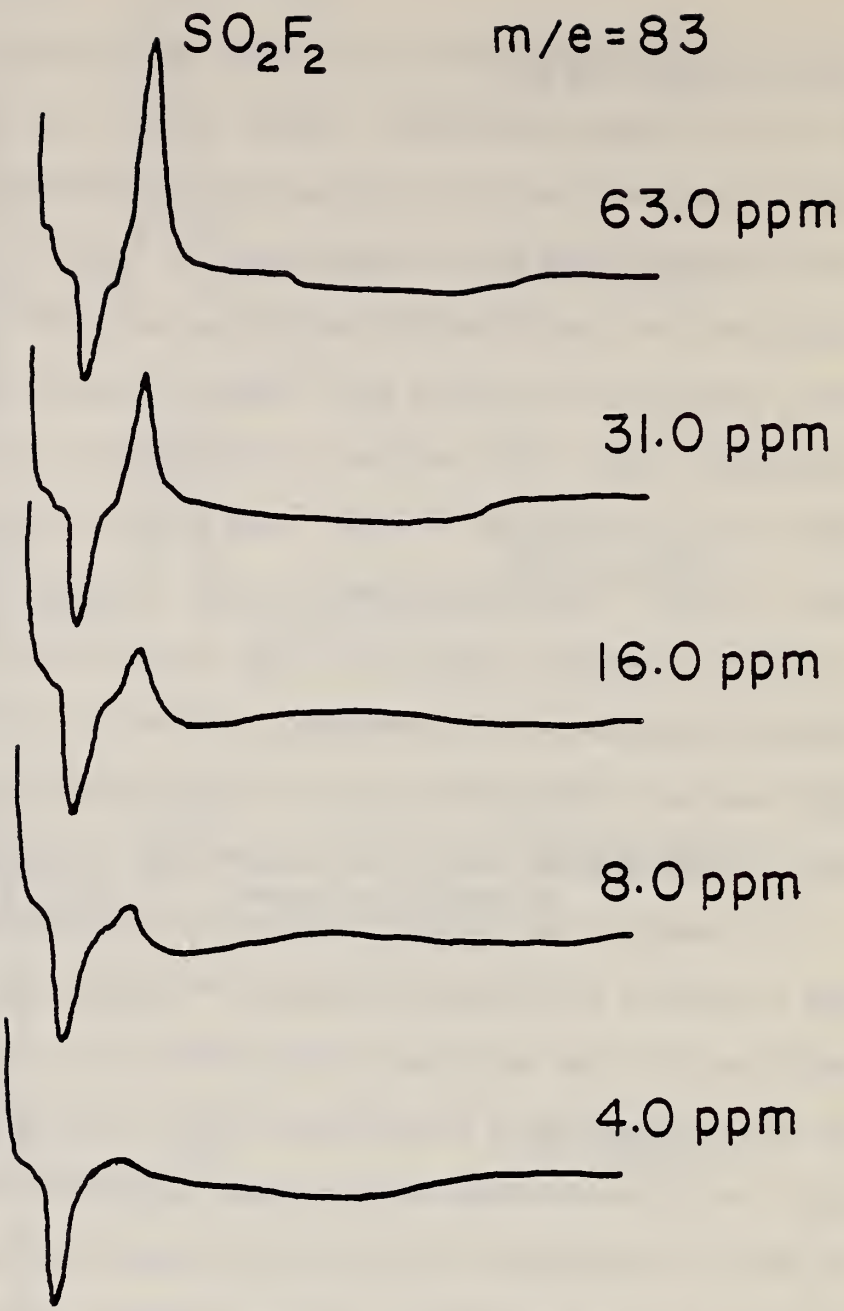

FIGURE 19. Single ion chromatograms for ion mass-to-charge ratio of 83 from gas samples containing the indicated concentrations of SO_2F^+ peak from SO_2F_2 and a dip in background associated with passage of SF_6 through the column.

SF_6 supply was initially free of SOF_2 and SO_2F_2 at the ppm level, the results of our analysis indicated that this was most likely the case. The ion chromatograms shown in Figs. 18 and 19 were obtained in analysis of the standard samples prepared by the method described above.

In addition to the checks mentioned above on proportionality of response to sample concentration, measurements were also made to check on proportionality of GC/MS response to sample volume. For example, the areas under the m/e = 70 peaks of SF_6 for 0.4 mL and 0.2 mL injections at the same concentration were compared. If the response is linear, the signal from the 0.4 mL sample should be twice that of the 0.2 mL sample. An average of more than five such comparisons, however, showed that the response ratio was (18 ± 6) percent higher than the expected value of 2.0. Comparing the areas under the m/e = 86 peaks for SOF_2 in 1.0 mL and 0.4 mL injections gave a ratio of these which was (9 ± 11) percent less than the expected value of 2.5. A similar comparison of peak heights for m/e = 102 from SO_2F_2 showed a ratio (33 ± 11) percent lower than 2.5; and finally, comparison of area under the m/e = 18 peak of H_2O gave ratios (20 ± 13) percent smaller than the actual volume ratios. These tests demonstrate that the response of the system is, in general, nonlinear with respect to volume of gas injected. It is speculated that this problem is most likely due to either nonlinearities in the efficiency of the membrane separator to passage of polar molecules, or consumption of gas in the process of column conditioning. The results of this test provide an indication of the relative error that would be introduced in comparing samples of

different sizes. To avoid this error, comparisons were made using samples having the same injection volume.

Measurements were also performed to check on the constancy of the GC/MS response to repeated injections of identical samples. In one test, 8 samples of 0.2 mL of SF_6 injected 1.5 minutes apart yielded responses uniform to 2 percent (one standard deviation), and 8 samples of 0.4 mL of SF_6 at various times throughout one day yielded the same response to 4 percent. There exists evidence, however, that the reproducibility is not always as good as is suggested by these results. At the present time, we have not undertaken a thorough investigation of all possible sources of error that might contribute to uncertainties in quantitative analysis using the GC/MS. It is our conservative estimate that the trace concentration levels reported here are accurate to within ±30 percent. A significant source of error might be associated with nonuniformity of trace contaminant concentrations within the corona cell. This could be reduced using improved gas sampling procedures. Further investigations of this are now underway.

In acquiring the data, the mass spectrometer was usually programmed to monitor preselected ions with the following m/e (mass-to-charge ratio): 16, 18 (indicative of H_2O); 64, 48, (SO_2); 32, 70 (O_2, SF_2, SF_4); 67, 86 (SOF_2); 83, 102 (SO_2F_2); 105 (SOF_4). In some cases, other ions were included when it became evident that other species such as OCS, CO_2, CO and CF_4 might be present. In the determination of absolute concentration levels, the areas under the ion chromatogram peaks were compared with those for the standard gas samples. This was done, for example, using the relationship

$$\frac{[\text{moles of } SOF_2/\text{moles of } SF_6] \text{ unknown}}{[\text{moles of } SOF_2/\text{moles } SF_6] \text{ calib.}} = \frac{[A(86)/A(70)] \text{ unknown}}{[A(86)/A(70)] \text{ calib.}},$$

where A(86) is the area under the m/e=86 chromatogram peak for SOF_2 and A(70) is the corresponding area for the m/e=70 ion from SF_6.

Usually the H_2O ions (m/e=16, 18), SF_6 ions (m/e=32, 70), and SOF_2 ion (m/e=86) were integrable by the data processor, whereas SOF_2 (m/e=67) and SO_2F_2 (m/e=83, 102) had to be measured by hand from plots. In the latter cases, areas could be accurately estimated from knowledge of peak heights and widths provided there was sufficient signal. For each of the species listed there are responses in two (or more) ion channels, of which one was more reliable by virtue of greater size or a steadier baseline and these were: for H_2O, m/e=18; SF_6, m/e=70; SOF_2, m/e=86; SO_2F_2, m/e=102.

II.C.3 Results

Figures 20 and 21 show single ion chromatograms for samples of SF_6 degraded by dc positive point-plane corona at a constant current of 2.0 μA. Indicated are the accumulated times during which the discharge was on. The SF_6 gas pressure for the measurements was 300 kPa (∿3 atm). Stainless-steel electrodes were used with a gap spacing of 1.27 cm and an initial point diameter of 0.16 mm. At the end of 32.5 hours of corona the point electrode was examined under a microscope. The tip, in addition to being discolored, had

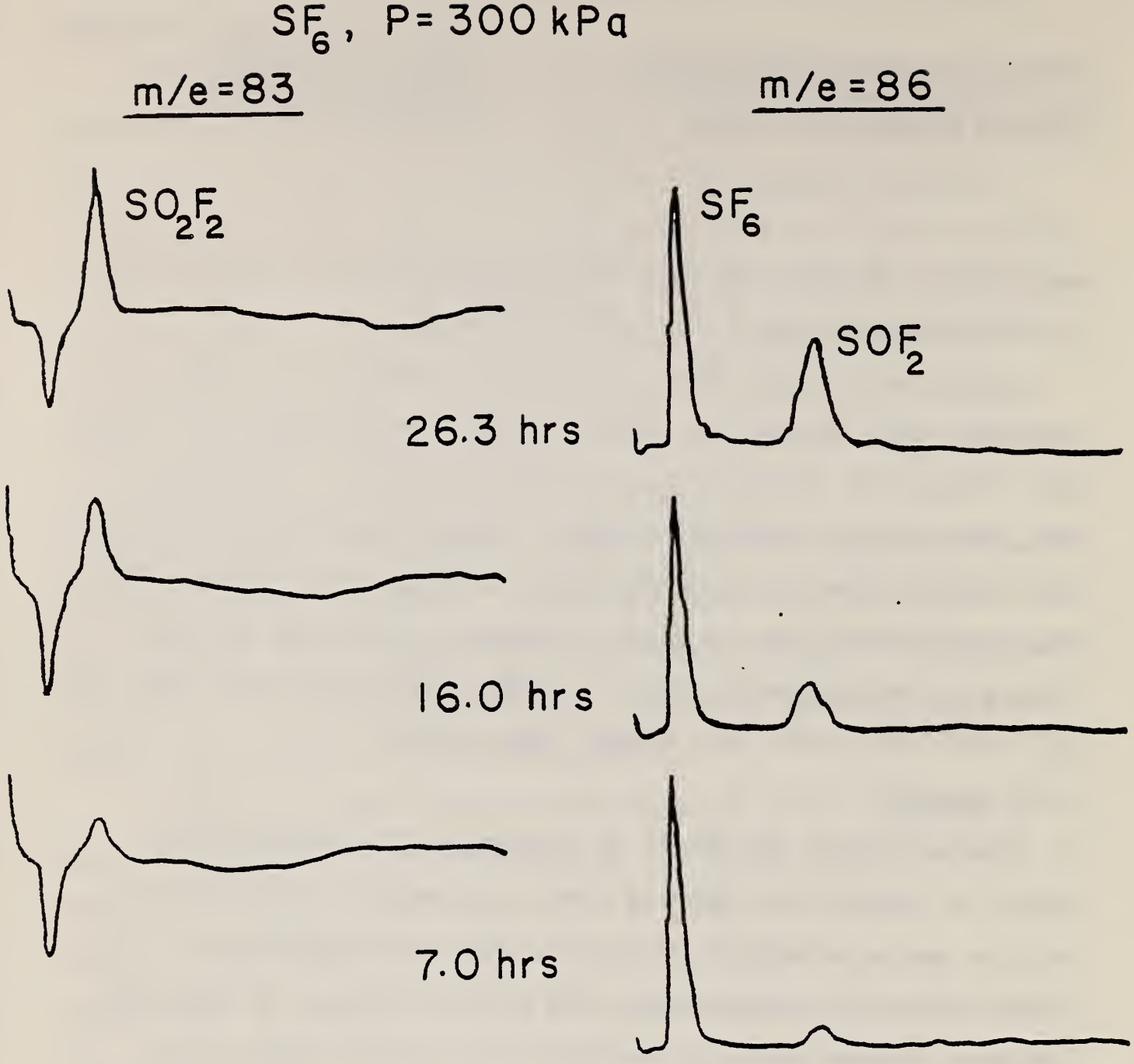

FIGURE 20. Single-ion chromatograms for ions of mass-to-charge ratios of 83 and 86 obtained from gas samples extracted after the indicated accumulated times during which SF_6 at an absolute pressure of 300 kPa was subjected to continuous positive dc corona at a constant current level of 2.0 μA. Shown are features associated with SF_6, SOF_2, and SO_2F_2.

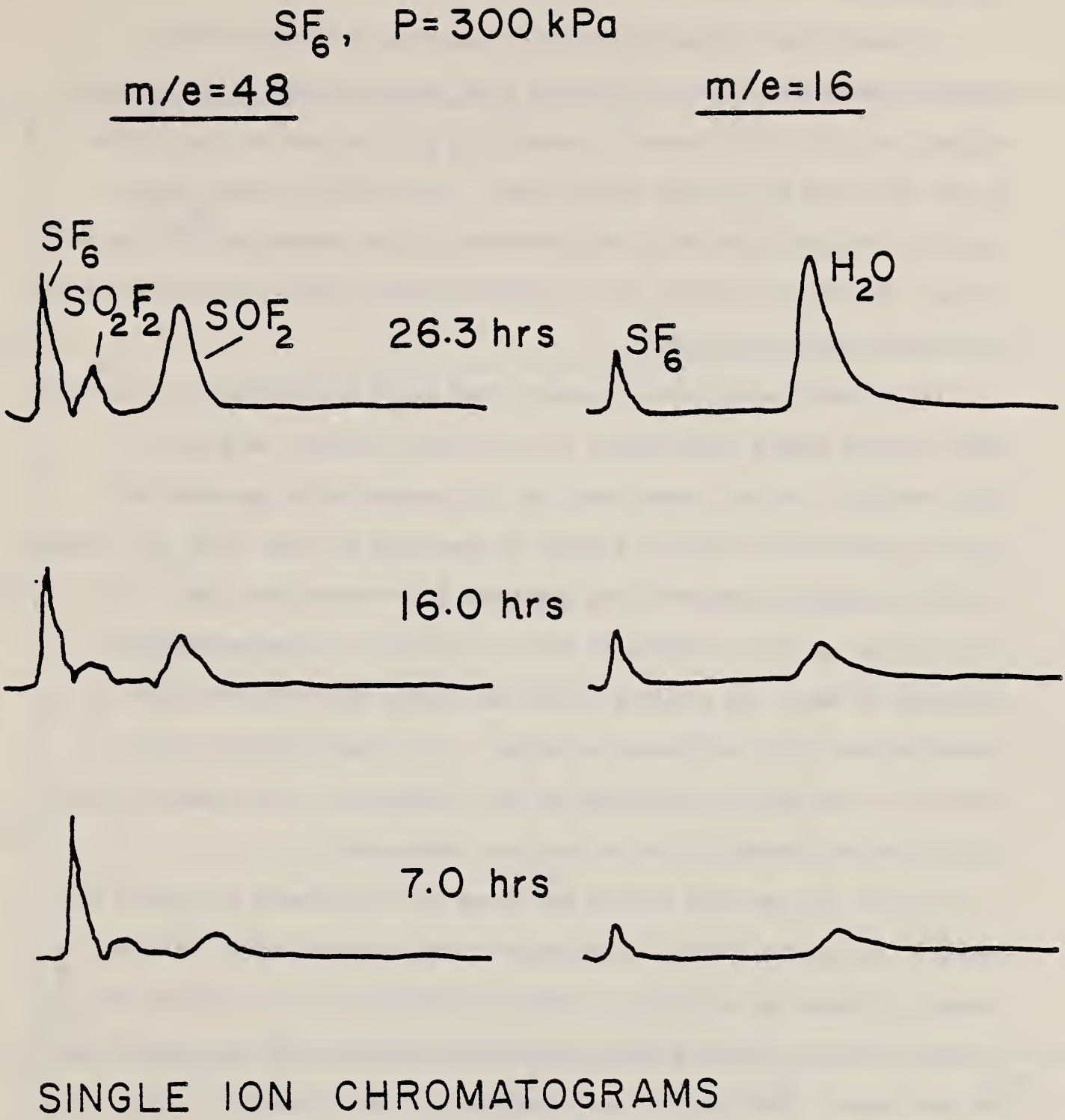

FIGURE 21. Single ion chromatograms for ions of mass-to-charge ratios of 16 and 48 obtained from gas samples extracted after the indicated accumulat times during which SF_6 at an absolute pressure of 300 kPa was subjected to continuous positive dc corona at a constant current level of 2.0 μA. Shown are features corresponding to SF_6, SO_2F_2, SOF_2 and H_2O.

increased in diameter by about 12 percent, thus indicating that some melting had occurred.

A direct visual comparison of the relative peak heights in the chromatograms shown in Figs. 20 and 21 with those in Figs. 18 and 19 would suggest that after 26.3 hours of corona, SO_2F_2 is present at roughly the 40 ppm level and SOF_2 at the 20 ppm level. The results of more careful analysis are consistent with these estimates giving respectively 39 ppm and 16 ppm. In the case of H_2O, only relative concentrations could be determined for reasons previously noted.

The primary decomposition products that could be observed with the GC/MS, after running corona continuously at 2.0 μA for 32 hours, were SOF_2, SO_2F_2 and H_2O. In this experiment, the H_2O concentration appeared to build up within the first 10-15 hours of operation and then level off, whereas the SOF_2 and SO_2F_2 concentrations continued to increase with time. This is indicated by the data shown in Figs. 22 and 23. In the measurements performed to date, the presence of H_2O was always the first indicator of contamination in SF_6 subjected to corona. It is speculated that H_2O is driven into the cell by the effect of the discharge in, for example, heating the electrode surfaces by ion or electron bombardment.

In Fig. 22, two sets of data are shown which represent an attempt to identify the source of H_2O. Starting with new electrodes that had been recently cleaned and polished, a corona discharge was run in 300 kPa SF_6, at a level of 2.0 μA, for 7.4 hours, and during this time the build-up of H_2O was monitored. Then the cell was evacuated to high vacuum and a fresh, dry SF_6 sample was introduced, again at a pressure of 300 kPa. Analysis of the

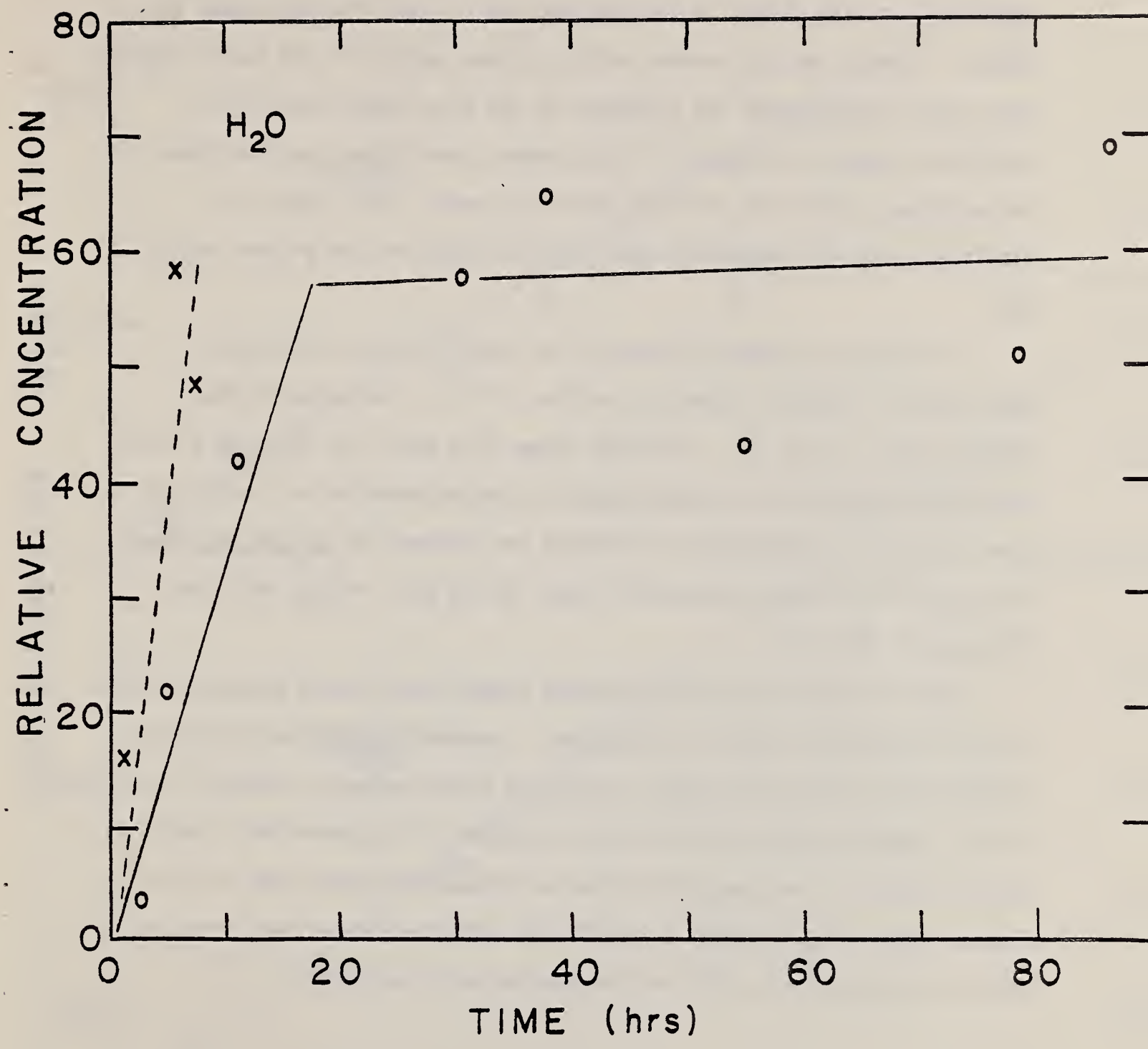

FIGURE 22. Time dependence of relative H_2O concentration in SF_6 at 300 kPa which had subjected to continuous positive dc corona discharges at a level of 2.0 μA. For the data corresponding to the x's "clean" electrodes were used, whereas for the data corresponding to the o's the electrodes had been preconditioned by prior discharges in SF_6.

new gas revealed no H_2O content. The corona discharge was then resumed at the same level and again the relative H_2O concentration was monitored as a function of time. In Fig. 22, the x's correspond to the initial discharge which was run with "clean" electrodes and the o's are from the second gas sample. Clearly the H_2O content builds up less rapidly in the second sample, which would suggest that the discharge in the first sample drove off a significant amount of H_2O and, in that sense, conditioned the electrodes for the subsequent test with the next fresh SF_6 sample. This result is consistent with the suggestion that the electrodes are the primary source of H_2O.

For times up to about 100 hours, the concentrations of SOF_2 and SO_2F_2 seem to increase linearly with time. This is indicated by the results shown in Fig. 23. For times longer than about 100 hours at 2.0 μA, additional decomposition products begin to become detectable. In Fig. 24, we show single ion chromatograms indicating the presence of SO_2 and OCS after 333 hours of continuous corona at a level of 2.0 μA. The SO_2 was first detected at 160 hours.

After 333 hours the point electrode showed considerable erosion which was visible without the aid of a microscope. Examination under the microscope revealed the presence of several nodules of yellow material, possibly pure sulfur, deposited near the tip of the electrode. Also after this time the quartz window on the side port of the cell showed definite signs of being etched, thus indicating that a significant amount of HF had been produced, which as noted before, could not be detected with the GC/MS.

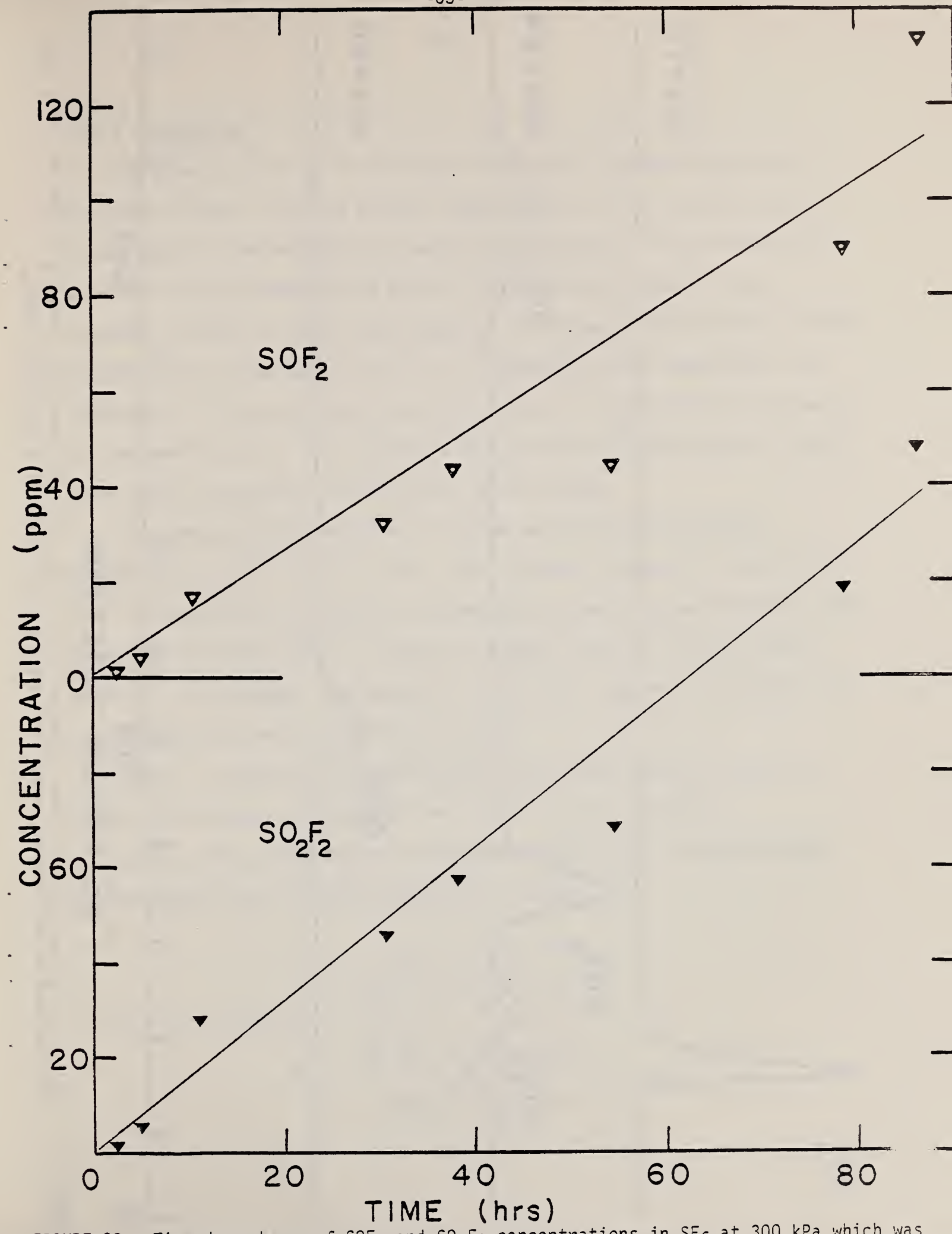

FIGURE 23. Time dependence of SOF_2 and SO_2F_2 concentrations in SF_6 at 300 kPa which was subjected to continuous positive dc corona at a level of 2.0 μA.

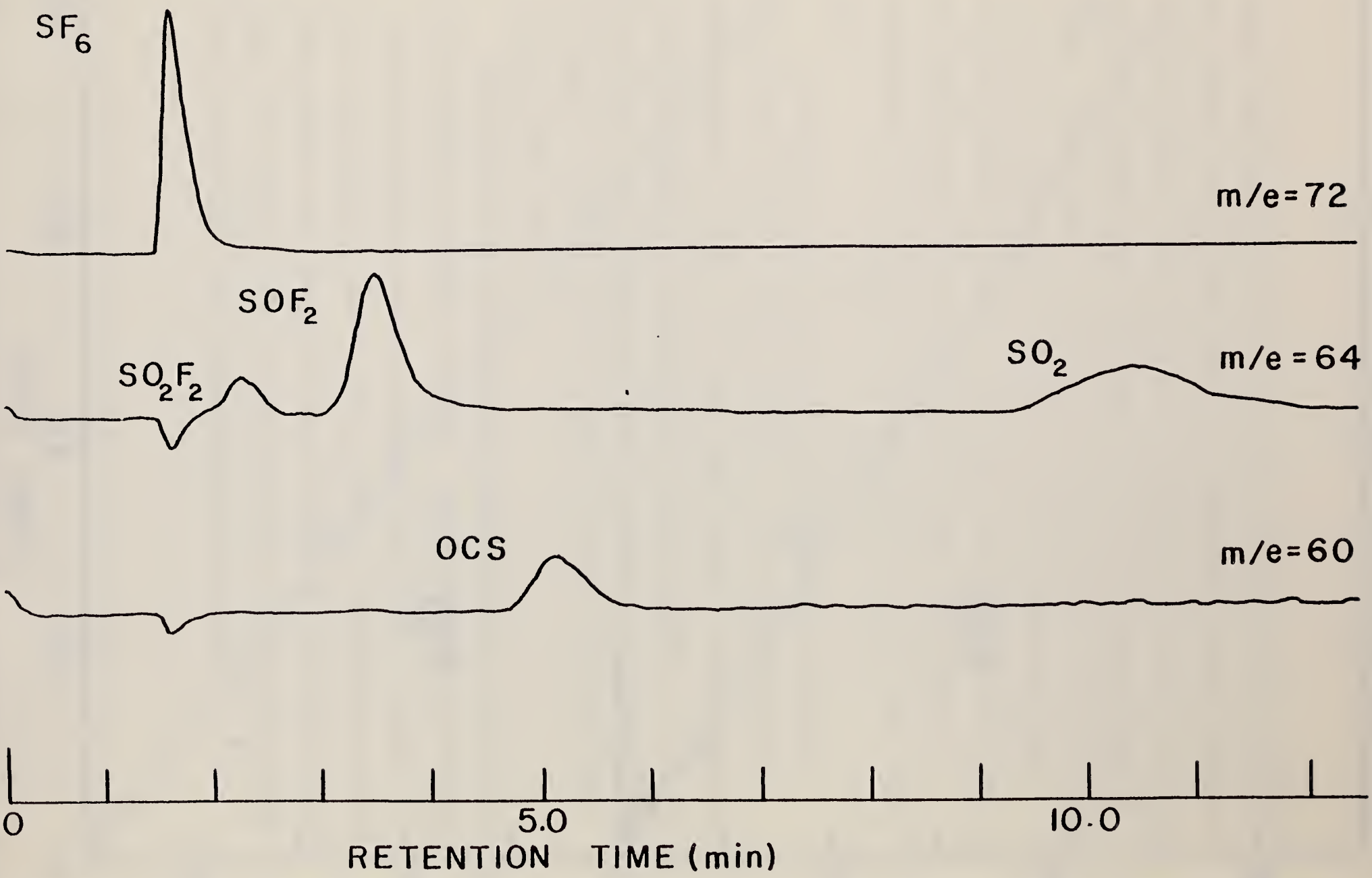

FIGURE 24. Single ion chromatograms for ions characteristic of SO_2, OCS, SOF_2 and SO_2F_2 from SF_6 at 300 kPa which had been degraded in positive dc corona for a period of 333 hours at a level of 2.0 μA.

II.C.4 Discussion

The production of H_2O in the corona discharge is somewhat surprising. The results shown in Fig. 22 strongly suggest that it is driven into the cell by the action of the discharge in heating the electrode. These results also show that the H_2O concentration tends to level off after several hours, presumably because an equilibrium condition is reached in which water is driven from the point at the same rate as it is consumed by other mechanisms, e.g., reabsorption. Also, the rate of water production is significantly affected by the preconditioning of the electrode with operation of a discharge for several hours before introducing the gas sample to be studied.

These measurements imply that it may be quite difficult to avoid introduction of H_2O into a test cell used to measure breakdown or study long time "aging" effects in corona. A further implication of these findings is that if partial discharges occur in practical systems insulated with gas, water vapor will be produced. The amount will, of course, depend on the duration of the discharge and area over which it occurs.

Water, if present, will significantly affect the chemistry that occurs during and subsequent to decomposition of the gas in a discharge.

In SF_6, free oxygen results from dissociation of H_2O in the discharge, and one expects the following reactions[22] to occur:

inside of the discharge

$$\begin{cases} SF_6 \xrightarrow{O} SOF_2 + 4F \\ SF_6 \xrightarrow{O} SOF_4 + 2F \\ SF_6 \rightarrow SF_4 + 2F \\ SOF_4 \xrightarrow{O} SO_2F_2 + 2F \ . \end{cases}$$

Outside the discharge region, SF_4 and SOF_4 will eventually hydrolyze in the presence of H_2O and be converted to SOF_2, SO_2F_2 and HF via the reactions

$$\text{outside of the discharge} \begin{cases} SF_4 + H_2O \rightarrow SOF_2 + 2HF \\ \\ SOF_4 + H_2O \rightarrow SO_2F_2 + 2HF. \end{cases}$$

In this way, we can explain the occurrence of SO_2F_2 and SOF_2 as predominant, observable, end decomposition products.

The fact that there was no evidence of HF, SF_4 or SOF_4 from analysis reported here is not sufficient basis for concluding that these compounds were not present. As noted before, these are very reactive gases and will not readily pass through the GC column used. In an attempt to evaluate the sensitivity of our GC/MS to detection of SF_4 in both N_2 and SF_6, no ions were observed in the mass spectrometer that could be directly attributed to SF_4. Instead we observed features corresponding to SOF_2 which we assume came largely from hydrolysis of SF_4 with trace amounts of H_2O in the mixing vessel or gas sampling syringe.

The mechanisms that account for production of SO_2 and OCS, which became detectable much later than the oxyfluorides, are not understood at this time. The appearance of these seemed to be associated with an apparent build up of CO, CO_2, and CF_4 concentrations, but further investigation of this is

required. It is clear though that SO_2 and OCS cannot result from primary decomposition of SF_6, and must involve secondary reactions, perhaps on the electrode surface. The source of carbon is not immediately obvious, although it might come directly from evaporation of the stainless-steel electrode. As noted, considerable deterioration of the electrode was evident.

The concentrations of the oxyfluorides seem to increase linearly with time as suggested by the data in Fig. 23. It would be desirable to observe in future experiments how the rate of production of these species depends on discharge power level. One might speculate that the slopes of the production curves should increase in proportion to the power level.

II.D. Effects of Trace Decomposition Products and H_2O on SF_6 Positive DC Corona Characteristics

II.D.1 Motivation

At the present time, we know of no other systematic studies of the effects of trace contaminants, such as H_2O, on the behavior of low level electric discharges in compressed SF_6. There is reason to suspect, as previously noted[2] in our study of corona in SF_6/N_2 mixtures, that the pulse characteristics of corona are quite sensitive to small changes in gas composition. In fact, a measurement of corona pulse characteristics might prove to be a useful diagnostic of insulation deterioration. This idea has been pursued already in earlier work.[12,14] In particular, measurement of changes in pulse height distributions (PHD's) might be one of the most sensitive indicators of contamination or deterioration.

It is, moreover, desirable to learn about the effect that trace contamination can have on corona inception and breakdown measurements used for

evaluation of dielectric performance of gases. This information could prove useful in the design of tests. If, for example, in performing a series of breakdown measurements, the first event alters the gas composition, then subsequent measurements with the same sample might be affected. Furthermore, it would be desirable to know, on a relative scale, how susceptible various gaseous dielectrics are to the presence of contamination as compared, for example, to SF_6. Some gases can be expected to be more resistant than others.

In the work described here, we have monitored the PHD's of partial discharges as a function of time for continuous dc corona in SF_6 under conditions of both constant current and constant voltage. At the same time, the content of the gas sample was monitored using a gas chromatograph/mass spectrometer (GC/MS). Experiments were also performed in which PHD characteristics of degraded gas were compared with those of a fresh gas sample under the same electrode conditions. In another experiment, pure SF_6 gas samples were artificially contaminated with trace amounts of H_2O using a hot wire technique, and the effects on the PHD and pulse repetition rates of the corona were noted. Preliminary results have already been reported.[3]

II.D.2 Measurements and Data

The PHD and pulse repetition rate measurements for SF_6 corona were performed using the multichannel analyzer system previously discussed in Sec. IIA (see Figs. 1 and 2). The chemical analysis of the gas was performed with the GC/MS and corresponding operating and sampling conditions described in the previous section. The relative concentration of H_2O and the absolute

concentrations of the oxyfluorides SOF_2 and SO_2F_2 were determined by the technique of single-ion monitoring (see previous section, also Ref. 31).

Figure 25 shows changes that occur in the positive corona PHD spectra as a function of time when SF_6 at a pressure of 200 kPa in a volume of 3780 cm^3 is subjected to continuous corona discharges for a period up to 260 minutes at constant voltage. Stainless-steel electrodes were used with a point-to-plane gap spacing of 2.28 cm and an initial point diameter of 0.09 mm. Also indicated in the figure are the corresponding average corona current and partial discharge repetition rates. The decreases in current and repetition rate are suspected to be associated mainly with changes in point electrode conditions. Some melting of the tip was, for example, evident after several hours of operation giving rise to an effective increase in tip diameter.

The changes in PHD seen in Fig. 25, however, seem to be more indicative of permanent changes in gas composition caused by the discharge. The general tendency, observed in several tests of this type, is for the PHD's for positive dc corona to exhibit greater contribution from small single pulses, and relatively less contribution from bursts, as time progresses. This is also evident in measurements performed under conditions of constant corona current. It appears to suggest that there is a decreasing tendency for the positive corona to develop as pulse bursts as the gas becomes more "degraded."

The most convincing evidence that the corona characteristics are sensitive to gas contamination is provided by comparative PHD measurements performed immediately before and after changing from a degraded to a pure gas sample. In this way effects due to changing electrode conditions are minimized. In Fig. 26a is shown the measured PHD for a sample of SF_6 which has been

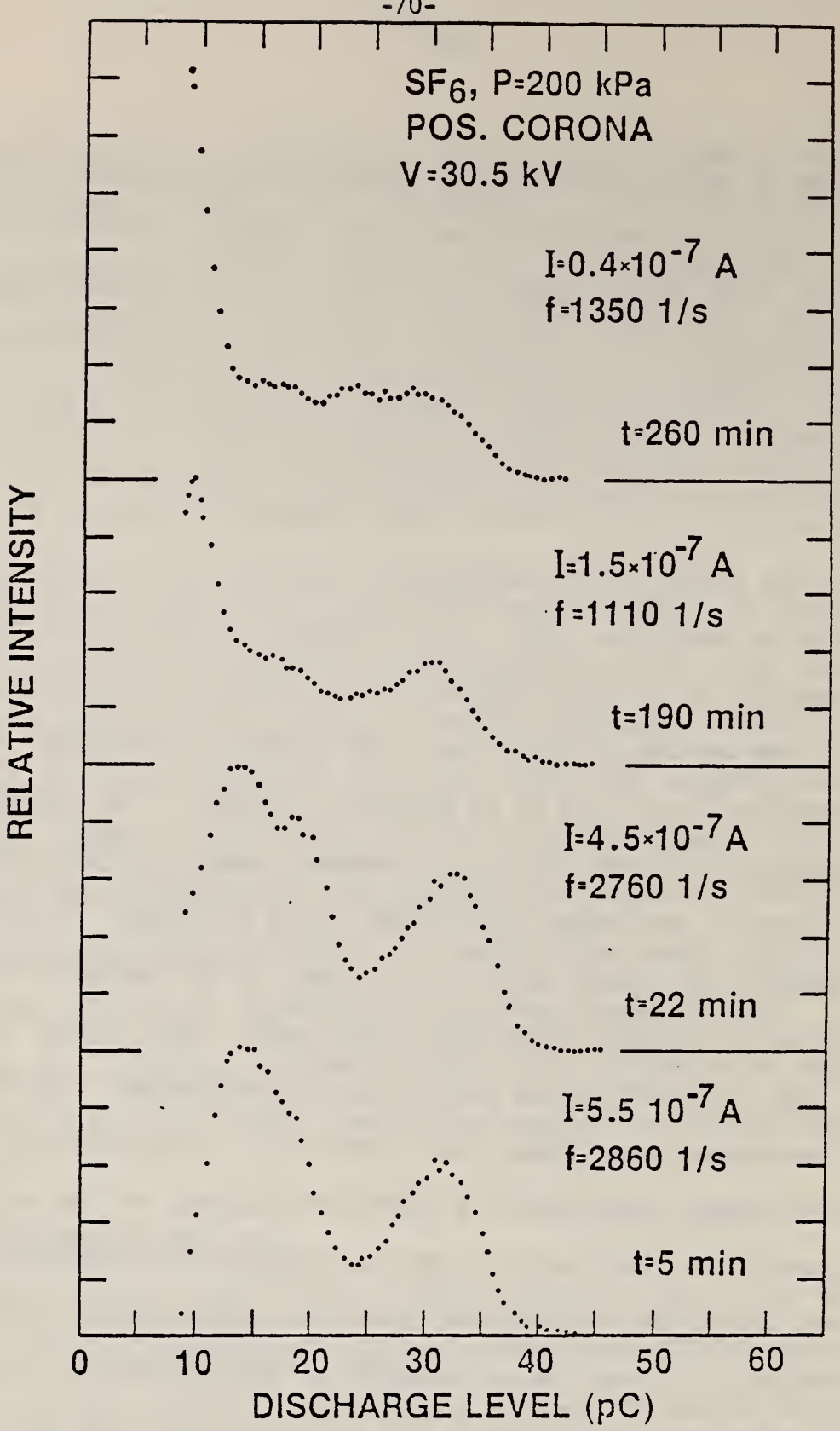

FIGURE 25. Time variation in partial discharge pulse height distribution for positive corona in SF_6 at a pressure of 200 kPa. Also indicated are corresponding average corona current and observed pulse repetition rates. The measurements were performed at a gap spacing of 2.28 cm with a point of diameter 0.09 mm, and a gas volume of 3780 cm^3.

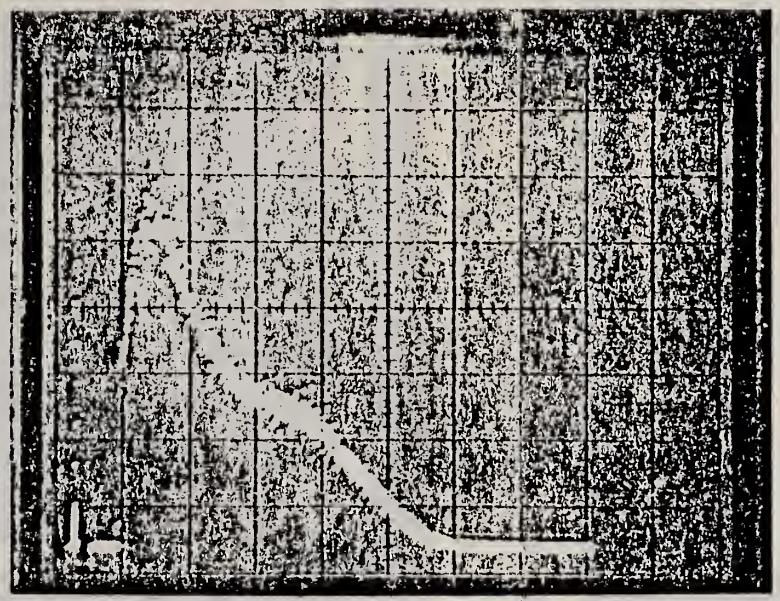

$I = 1.5 \times 10^{-6} A, \quad f = 6800/s$

a

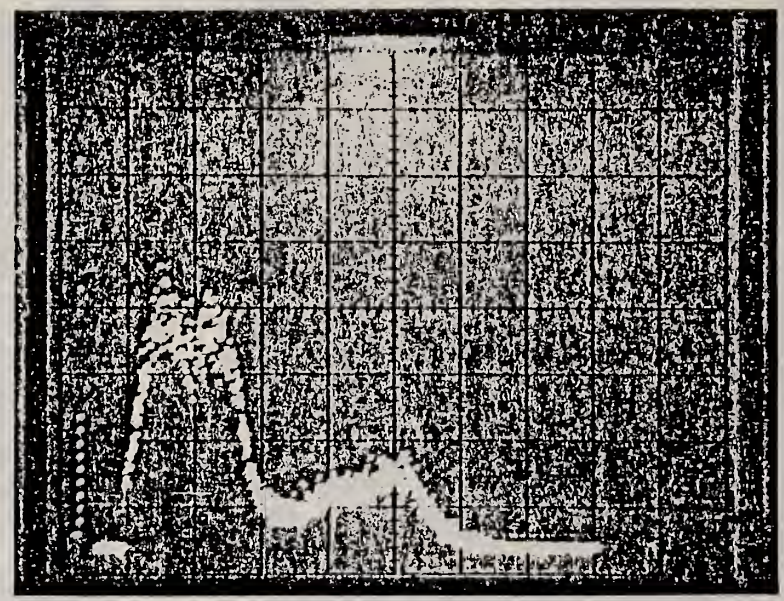

$I = 4.0 \times 10^{-8} A, \quad f = 39/s$

b

FIGURE 26. Partial discharge pulse height distributions for positive dc corona in SF_6 at an absolute gas pressure of 200 kPa and applied voltage of 46.6 kV for (a) gas degraded by corona at constant current of 1.5 μA for the period of 32 hours immediately before changing the sample, and for (b) pure SF_6 immediately after introducing a fresh gas sample. Indicated are the corresponding corona currents and pulse repetition rates. The charge level scale is the same for both displays.

degraded by corona at a constant current of 1.5 μA for a period of 32 hours. Immediately following this measurement, the cell was evacuated to high vacuum and a fresh sample of pure SF_6 was introduced at the same pressure (200 kPa) and the PHD was again measured at the same voltage of 46.6 kV. The result of the latter measurement is shown in Fig. 26b. Note that not only is there a dramatic difference in the PHD spectra, but also both the corona current and pulse repetition rate are down two orders of magnitude relative to the degraded sample. The tendency for pulse bursts to dominate is restored upon adding a fresh gas sample as indicated by the PHD (also compare Fig. 26 with Figs. 3, 4 and 25). In Fig. 27, we show oscilloscope traces illustrating how the initial burst characteristic of the discharges becomes more diffuse and separated with time and eventually gives way to a phenomenon dominated by single, isolated pulses. After 14.0 hours of corona, burst activity ceases.

During the same tests described above, gas samples were periodically extracted from the cell and analyzed with the GC/MS system. Such analysis was performed immediately after extraction with the syringe to avoid contamination from atmospheric constituents, primarily H_2O. The results of one such experiment which ran for 32.5 hours are shown in Fig. 28. It should be noted that the pulses shown in Fig. 27 correspond to this particular experiment. For this case, a positive dc corona was operated at a constant current of 2.0 μA in SF_6 at an initial absolute pressure of 300 kPa (∿3 atm). Stainless steel point-plane electrodes were used with a gap spacing of 1.27 cm and an initial point diameter of 0.16 mm. The gas was contained in a 3780 cm^3 volume. At the end of 32.5 hours the point electrode was examined and the tip, in addition to being discolored as usual, was found to have increased in diameter by

SF_6 CORONA PULSES

t = 0.0hrs

t = 9.0 hrs

t = 14.0hrs

FIGURE 27. Changes in observed positive corona pulse shapes in SF_6 corresponding to the experiment which yielded the data in Figure 28.

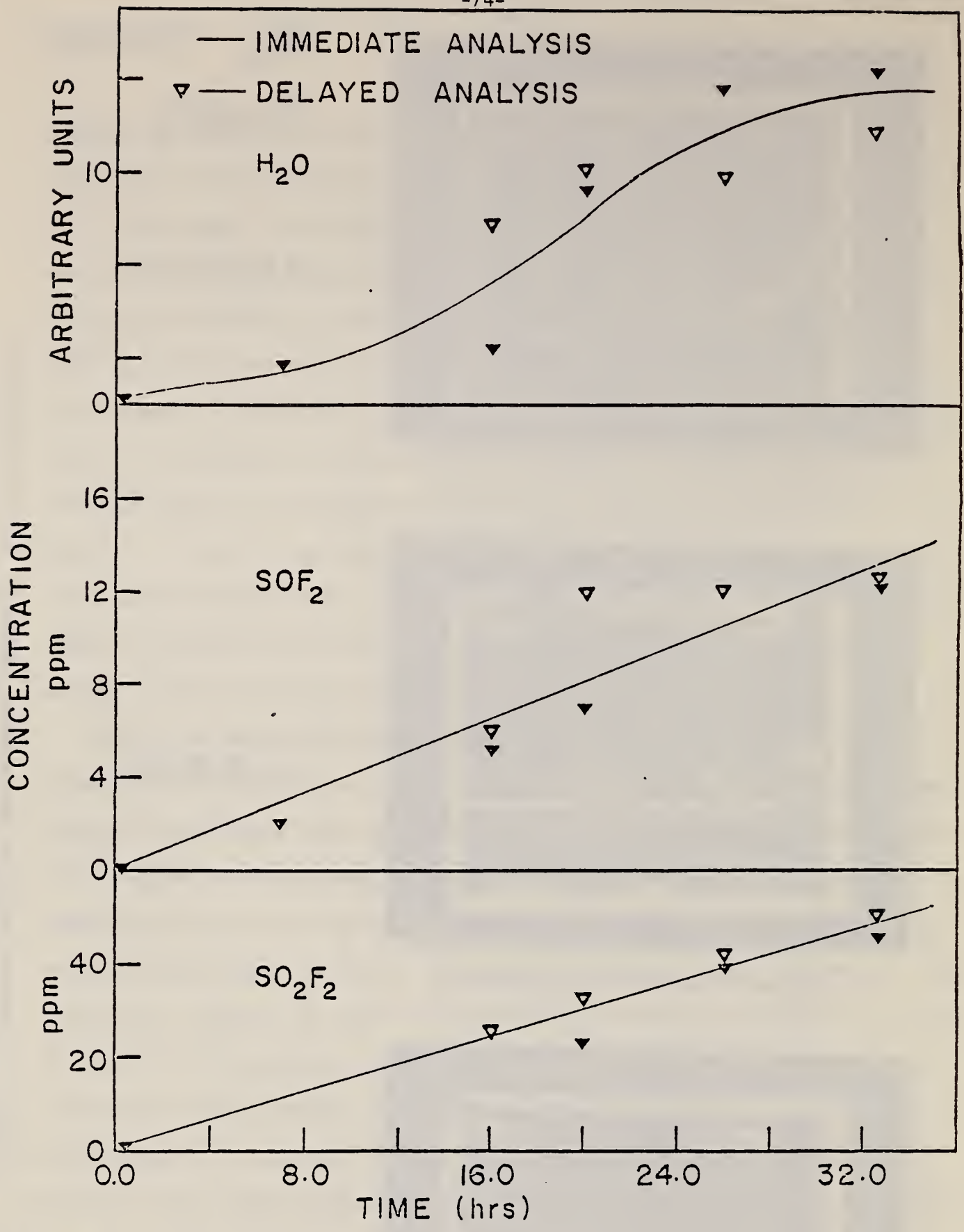

FIGURE 28. Time dependence of measured concentrations of H_2O, SOF_2, and SO_2F_2 in SF_6 at 300 kPa which had been subjected to continuous positive dc corona discharges at a level of 2.0 μA. Shown are data obtained from analyses performed immediately after the corona was turned off and from analysis after corona had been off for three or more hours.

12 percent, thus indicating that some melting had occurred. The effect of melting in this case, however, was not nearly as severe as it was for the sharper point used to obtain data presented in Fig. 25. For the experiment considered here, it was not necessary to turn up the voltage with time to maintain constant current. In fact, the required voltage actually decreased slightly from 32.8 kV initially to 27.7 kV at the time the experiment was terminated thereby demonstrating that effects of electrode melting can be significantly reduced by using larger electrode tip diameters and higher operating voltages.

Two sets of data are shown in Fig. 28; one corresponding to analysis performed immediately after the corona was turned off, and the other corresponding to analysis performed after the corona had been off for several hours so that the gas had ample time to equilibrate. On the basis of this rather limited data, it would not be possible to conclude that there are significant, systematic differences between the results obtained from these two sampling procedures, although in a few cases there are clearly large differences.

Again like the data shown in Figs. 22 and 23, the oxyfluoride concentrations seem to be increasing nearly linearly with time, and the H_2O concentration shows evidence of reaching saturation. It is significant to point out from a comparison of Figs. 27 and 28 that, by the time that there is a pronounced change in pulse characteristics of the positive corona, the concentration of SOF_2 is only about 4 ppm and that for SO_2F_2 is only about 15 ppm. Even keeping in mind the possible 30 percent uncertainty in

these values, it is remarkable that such a large change in discharge behavior can be associated with such small increases in contaminant concentrations.

The experiments on the effect of trace gaseous decomposition products on corona were followed by experiments in which H_2O was deliberately introduced into samples of pure SF_6. Evidence from the degradation experiments described above suggests that the presence of small amounts of H_2O could have a large effect on corona. In these experiments, water was injected into a cell containing pressurized SF_6 by heating a wire. Two wires were used in separate experiments. One was a stainless steel wire having a diameter of 0.06 mm and length of 30 cm and the other was a nichrome wire having a diameter of 0.051 cm and a length of 20 cm. In both experiments, while the wires were heated for several hours by passing a constant current through them, the build up of H_2O in the cell was monitored with the GC/MS. The results are shown in Fig. 29. For the stainless steel wire, the SF_6 pressure was 300 kPa and, for the nichrome wire, it was 200 kPa. It is seen that the rate of H_2O injection from both types of wires is similar. Both exhibit a saturation effect similar to that which occurs when H_2O is produced by running the corona discharge. This observation lends further support to the hypothesis (see the previous section) that in the operation of a discharge, H_2O is driven into the cell by local heating of the electrode.

To examine the effect of H_2O on positive dc corona, the electrical characteristics were determined at the following times: 1) immediately after a fresh SF_6 sample was introduced before injection of water, 2) after water was injected by heating the wires for roughly 15 hours (see Fig. 29), and 3) after the SF_6 sample contaminated by H_2O had been replaced with a fresh, pure

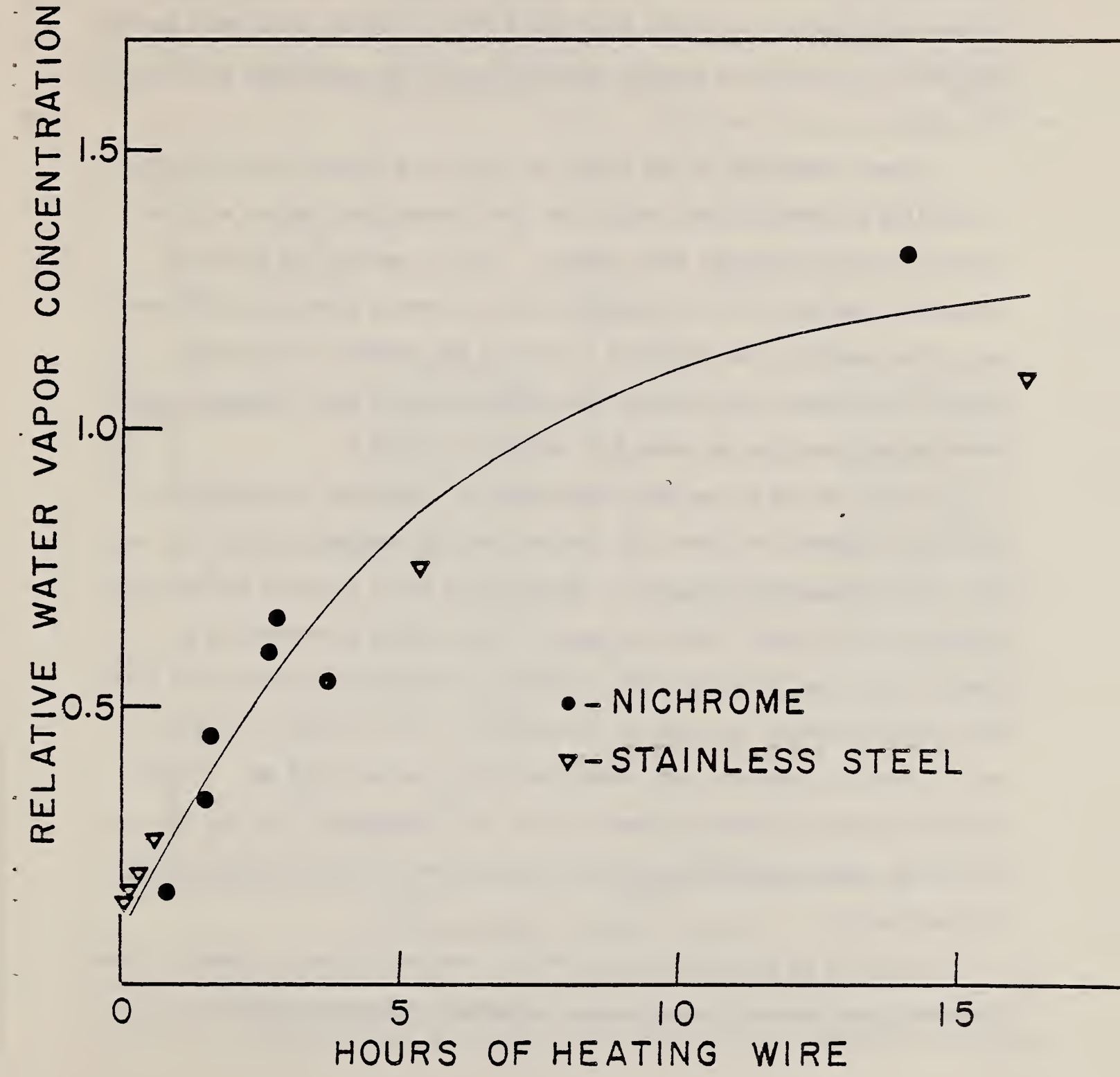

FIGURE 29. Time dependence of relative concentrations of H_2O vapor in SF_6 measured with a GC/MS for two experiments involving electrical heating of wires described in the text.

sample at the same pressure. The electrode conditions were the same in all cases since the discharge was run at a relatively low level for a short time sufficient to characterize it by performing PHD, pulse repetition rate, and current measurements (typically less than 5 min.). During these short periods the corona is unlikely to have noticeable effect on the electrodes (see data in Fig. 25).

The best indication of the effect of H_2O on the corona characteristics is obtained by comparing the results for the contaminated samples with the results for the subsequent fresh samples. This is because the total gas pressure in the cell will be reduced slightly (perhaps as much as 10 percent) due to the sampling with the GC/MS to monitor H_2O concentration during heating of the wire. It is known that even relatively small changes in gas pressure can give rise to detectable changes in corona.[2]

In Figs. 30 and 31, we show comparisons of electrical characteristics of SF_6 corona observed for fresh and contaminated gas samples. In Fig. 30, we also show corresponding single-ion chromatograms which indicate the relative concentrations of H_2O. The large peaks in these scans correspond to a feature associated with SF_6 which should be of comparable intensity for both gas samples assuming identical GC/MS conditions. For the data in Figs. 30 and 31, the tip diameters were respectively 0.12 mm and 0.096 mm. In both cases, the point-to-plane gap was 1.28 cm. For the data in Fig. 30, H_2O was introduced using the stainless steel wire, whereas for Fig. 31 the nichrome wire was used.

In Fig. 31 we show the observed PHD's, repetition rates f, average corona current I, and observed pulse shapes. A comparison between pure and

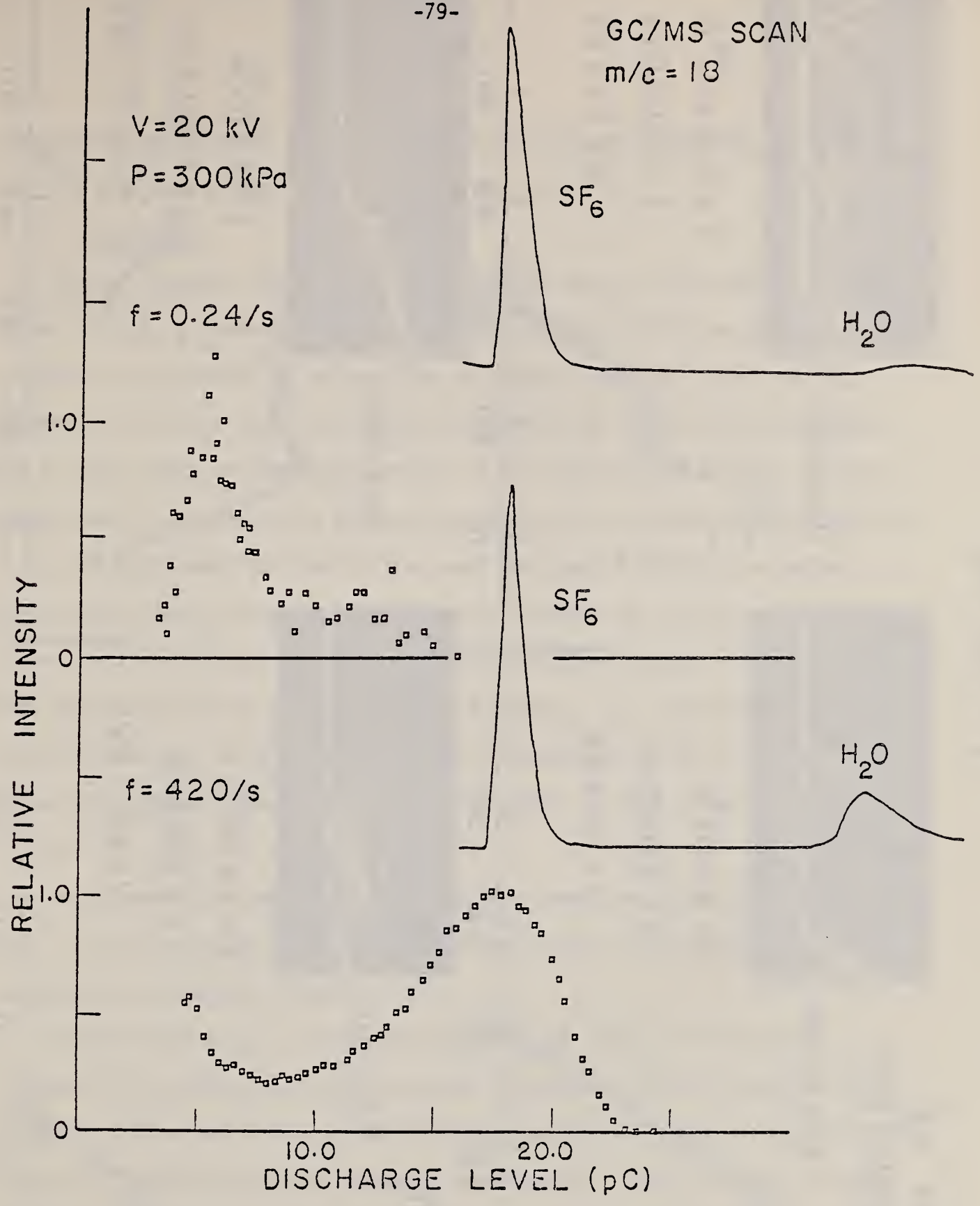

FIGURE 30. Pulse height distribution and frequency of positive dc corona in SF_6 at 300 kPa with and without trace H_2O contamination as indicated.

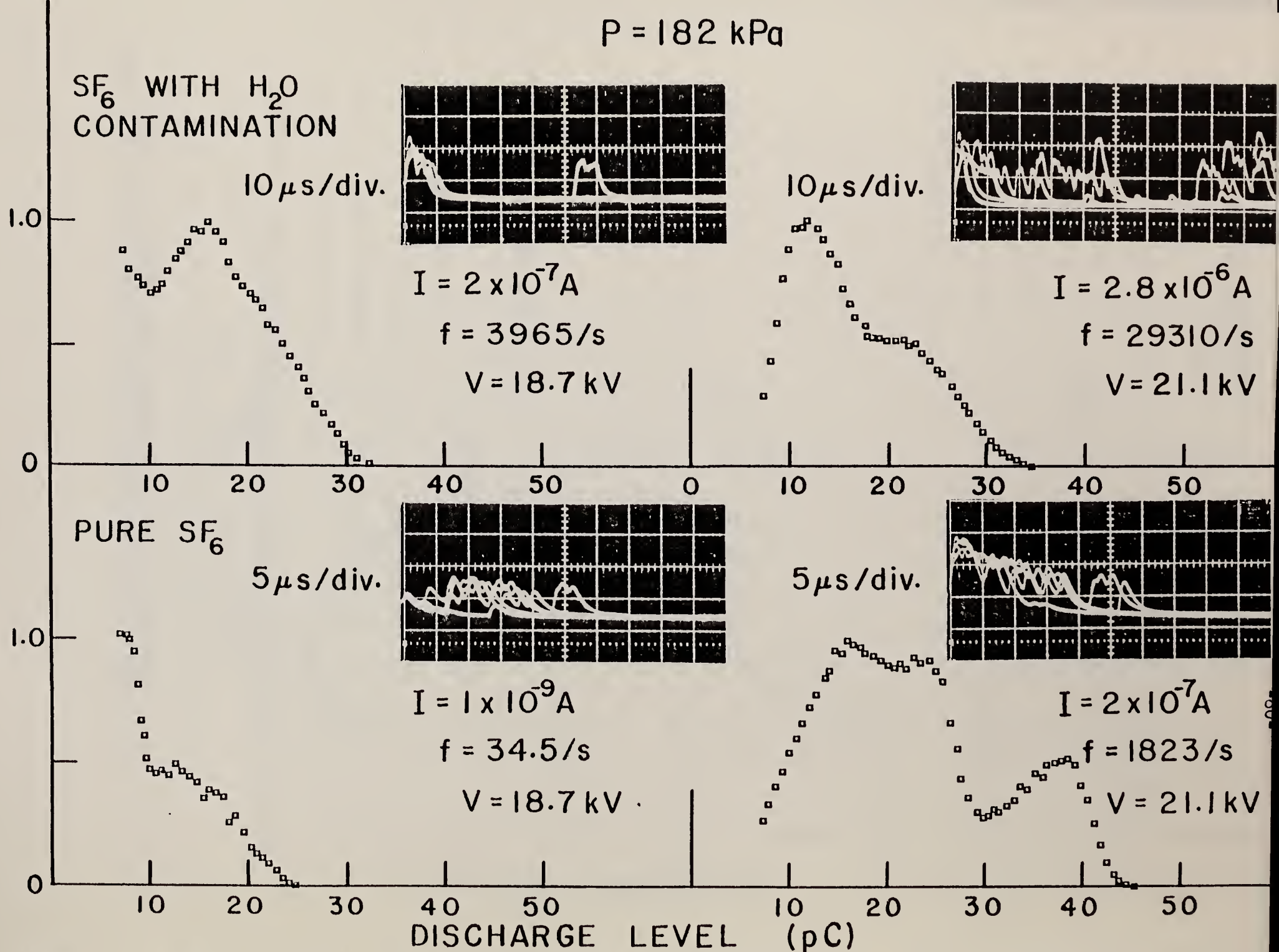

FIGURE 31. Comparison of electrical characteristics of positive dc corona in SF_6 at 182 kPa for indicated voltages and trace H_2O contamination.

contaminated gas samples is made at the same voltages, namely 18.7 kV and 21.1 kV, and at the same current, namely 2.0×10^{-7} A.

II.D.3 Discussion

As seen from the results given in Figs. 30 and 31, the presence of trace amounts of H_2O in compressed SF_6 can have an enormous effect on the electrical characteristics of positive dc corona. In Fig. 30, we see that, compared to the pure gas, the repetition rate of the corona for contaminated gas is four orders of magnitude greater at the same applied voltage of 20 kV. These results, together with those given in Fig. 31, indicate that the effect of H_2O is most dramatic close to the onset voltage, as might be expected. Water vapor clearly degrades the dielectric strength of the gas. The effect of H_2O on the PHD characteristics is seen to be similar to that which results from degradation of SF_6 in a continuous discharge, i.e., the presence of H_2O diminishes the tendency for the corona to develop as bursts. This is evident by comparing the before- and- after PHD's in Fig. 26 with those for 21.1 kV in Fig. 31.

On the basis of the information acquired here, one could presumably argue that it is H_2O that accounts for most of the change in PHD's when the gas is degraded by a discharge (see Fig. 25).

On the other hand, it could also be that the effect of the other decomposition products is similar to that of water. With the data that is presently available, it is not possible to separate the effect of H_2O from that of all other known trace gases in degraded SF_6. This is partly because, at the present time, it is not possible to perform a reliable quantitative analysis of H_2O content with the GC/MS. However, by comparison with the

results for other products, one might guess that the maximum absolute concentrations of H_2O in Figs. 28 and 29 are on the order of 100 ppm. Further work on this is required.

A meaningful quantitative comparison of the effects of H_2O and discharge-produced gaseous contaminants on corona behavior is not possible for other reasons. In the present experimental procedure there are, for example, no assurances that the electrode conditions are the same, since in the degradation experiment the corona characteristics are measured with the same electrodes used to operate the continuous discharge, and the point electrode is known to undergo some deterioration when the discharge is run for extended periods.

One can conclude, on the basis of the measurements reported here, that the presence of trace contaminants such as H_2O, SOF_2, SO_2F_2 and HF can have a large effect on the burst characteristics of positive dc corona in pressurized SF_6. The effect which H_2O and the other contaminants have in inhibiting burst activity can perhaps best be understood in terms of the influence that these molecules have on the development and dynamics of ionic space charge in the point-plane gap. As already noted in Sec. IIA (also see Refs. 10 and 11) the burst characteristics are controlled by the manner in which the positive ion space charge develops; thus anything that perturbs this space charge will likewise change the bursts. Unlike SF_6, the molecules H_2O, SOF_2, SO_2F_2 and HF are all polar, and polar molecules, particularly H_2O, have a tendency to form clusters around ions. Due to clustering, the positive ion mobilities in the gap will be decreased and this leads to an enhancement of the rate of positive space charge build-up near the point. A rapid increase in the positive space charge will tend to quench

secondary electron avalanche development and thereby inhibit bursts. Other processes such as charge transfer collisions could also affect ion mobilities and thus the way in which space charge develops.

The enhancement in the level of corona, i.e., pulse rate and average current, due to trace decomposition products and/or H_2O is most likely the result of an increase in the effective ionization coefficient of the gas. Insufficient information exists at this time however to determine if this explanation is realistic.

II.E. Laser Induced Changes in N_2 Corona Characteristics

II.E.1 Motivation

To our knowledge, the effect of intense optical laser beams on development and characteristics of corona discharges has not previously been investigated. The purpose of this work has been to evaluate the possibility of using the laser stimulated opto-galvanic effect as a microscopic diagnostic of fundamental processes in corona discharges. The idea is that by optically pumping selected atomic or molecular species with a tunable light beam incident on the discharge region one induces a change in the effective ionization coefficient of the gas, which manifests itself as a measurable change in discharge current. This kind of effect has been observed in several types of low pressure discharges, primarily hollow cathode discharges.[32-34]

It is also of interest to investigate the effect which laser light might have on modification of electrode conditions, e.g., via photon enhanced field emission. The N_2 discharge was chosen as the starting point for this exploratory investigation because it is one of the few molecular gases for which opto-galvanic signals have been reported.[33]

II.E.2 Experimental Arrangement

Working with a coaxial electrode system, an attempt was made to observe the opto-galvanic effect in N_2 with positive dc corona. The cylinder was fabricated from aluminum and the center corona wire was made of 5.7×10^{-3} cm diameter stainless steel wire. To obtain optimum sensitivity in this measurement, the coaxial electrode system was designed (see Fig. 32) to permit a dye-laser beam to be directed coaxially with the corona wire and into the visible glow of the corona. The measurements were carried out for the pressures ranging from 1.3 kPa (10 Torr) to 13.3 kPa (100 Torr). Laser powers typically near 100 mW were used, but smaller and greater powers were occasionally employed. The maximum discharge current was near 1.1 mA.

The beam from the dye laser was mechanically chopped with a rotating slotted disc and the in-phase component of the resulting change in discharge current was measured using a phase sensitive detector which employed a lock-in amplifier. The current was sensed as a voltage across a resistor in series with the discharge cell. Opto-galvanic signals observed with a neon-filled hollow-cathode lamp were used for wavelength calibration of the laser.

II.E.3 Results and Discussion

The opto-galvanic effect, in the form of discrete lines corresponding to electronic transitions in excited N_2 or N_2^+, was not observed for positive dc corona generated in this experiment. A change in corona current due to the presence of the incident laser light was detected, however. This signal, which was continuous, exhibited some wavelength dependence, and could, on occasion, be made to change polarity by changing the voltage applied to the cylinder. When the signal was positive, it decreased in magnitude as the

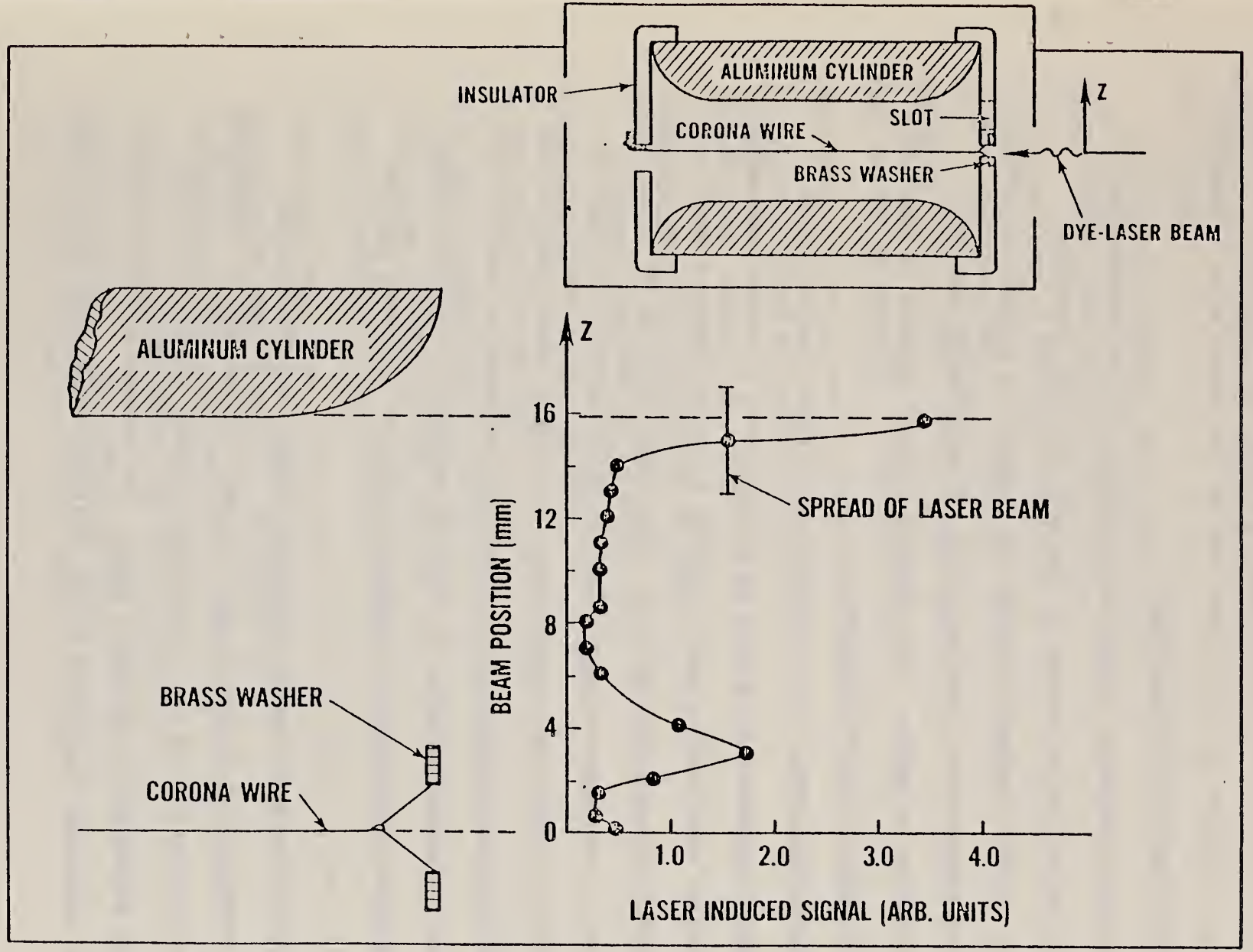

FIGURE 32. Change in corona current as a function of dye laser beam position. The data has not been corrected for a slow decrease in average discharge current.

wavelength was increased from 580 nm to 620 nm. When negative, the signal increased as the wavelength was increased. The effect was most pronounced when the laser beam was incident on the cylinder and not the corona wire. Figure 32 shows the spatial dependence of the effect.

The signal when observed as a function of time at a given wavelength is unstable and may be coupled to changes in the basic physical processes occurring in the partial discharge related, for example, to changes in surface conditions or gas composition. Reproducibility of measurements was, as a result, very difficult to achieve. The greatest signals appeared to occur near the breakdown voltage at a given pressure.

Because the maximum signal, as a function of position, occurs at the cylinder surface, it appears likely that we are observing a surface phenomenon. The cylinder surface does provide some electrons to the discharge process when positive ions and uv photons impinge on it. The laser light may be influencing this process, e.g., via photon-enhanced electric field emission, but such an interpretation is, at this time, speculative. In view of these results, and considering the importance which surface conditions are known to have in high field breakdown of compressed gases, it would be desirable to explore further the use of a tunable laser beam as a diagnostic probe of electrode surface conditions.

The results of the measurements performed suggest that the ordinary opto-galvanic effect, which is due in part to laser-induced optical pumping of metastables in a discharge, is not a particularly useful diagnostic in the study of corona discharges in molecular gases. The reasons for this are not entirely clear, but might be related to the relatively high noise level in most

corona discharges as well as the fact that molecular species are generally more effective in collisionally quenching metastables.

II.F. Other

During this reporting period there were several other activities and accomplishments that deserve mentioning. Minutes were prepared and distributed for the Workshop on Gaseous Dielectrics for Use in Future Electric-Power Systems which was held at the National Bureau of Standards on September 10-11, 1979.[6] These minutes were extracted from tape recordings made during the meeting. The workshop was held for the purpose of addressing questions concerning current and planned research on development of new gaseous dielectrics viewed as possible substitutes for SF_6. Focus was on identifying technological barriers to acceptable use of new gases and gas mixtures and questions concerning properties of gases in need of further investigation.

A report concerned with the safe handling of SF_6 used in laboratory type electrical apparatus was prepared.[7] This report is intended to benefit those within NBS who are not familiar with the properties of SF_6, but who must use this gas for electrical insulation or arc interruption. The information it contains was derived from the National Institute of Occupational Safety and Health's Registry of Toxic Effects of Chemical Substances and from other sources believed to be reliable, but is not the result of any critical data evaluation or testing activity performed at NBS. A report entitled "A Bibliography of Electron Swarm Data"[5] was completed and copies are now available for distribution from the JILA Atomic Collisions Data Center in Boulder, Colorado. This report allows a user to find electron swarm data (and some related information) in the regular literature. The types of data

included are for example: ionization, attachment, excitation, and recombination rates (or coefficients) for electrons in various atomic and molecular gases. Also included are data on electron drift velocities, energy distribution functions, diffusion and mobility. The bibliography is quite comprehensive and includes experimental and theoretical data on nearly all gases of interest as components in gaseous dielectrics, as well as for other applications where discharges are important, e.g., lasers, light sources, high voltage switches, etc. Copies of each of the papers listed have been saved on microfilm. A compilation of electron swarm data has also been completed and a report containing this data together with critical commentary is in preparation.

III. Conclusions and Summary

A measurement technique for quantitatively characterizing partial discharges for laboratory studies of gaseous dielectrics has been developed and evaluated. This technique provides a relatively complete description of the electrical properties of corona such as the pulse repetition rate, pulse height distribution, pulse shapes and average current. By this approach, one can obtain reproducible numerical data on corona which presumably can be compared with similar measurements in other laboratories. The instrument, which employs a relatively fast multichannel analyzer, has inherent limitations due to the finite sampling rate and time constants of the circuits involved. It is fast enough at present, however, to give a useful statistical signature of pulse shapes and pulse bursts. Possible problems in interpretation of pulse height distributions occur mainly when the corona pulse duration exceeds the RC time

constant of the detection circuit or when the mean interval between pulses, particularly in a burst, is small compared to the analyzer sampling time.

The pulse characteristics of dc corona in SF_6 and SF_6/N_2 mixtures were measured for a point-plane electrode geometry. It was discovered that these characteristics are quite sensitive to gas pressure, gas composition and applied voltage. There is also a very significant dependence of corona pulse characteristics on electrode polarity. The pulse height distributions were insensitive to irradiation of the gap with uv light, and the trends in voltage, pressure, and polarity dependence were relatively insensitive to changes in electrode gap spacing. This was not necessarily the case, however, for pulse repetition rates. At the larger gap spacings and higher pressures, for example, the positive dc corona pulse rate was seen to be very sensitive to uv radiation near onset. Negative corona pulse characteristics are more sensitive to point electrode conditions, whereas positive corona is more sensitive to gas composition.

It was discovered, in fact, that positive dc corona pulse height distributions are sensitive indicators of trace contamination in SF_6. When trace amounts of H_2O are introduced into pressurized SF_6, the burst activity in positive corona is found to be inhibited. This is also true after SF_6 has been degraded by continuous corona for several hours. In both cases, the level of corona increases with contaminant concentration indicating a reduction in dielectric strength. It is speculated that the changes in corona burst characteristics are related to the effect of polar molecules on development of positive ion space charge in the gap. The reduction in

dielectric strength is probably due to contaminant-induced changes in the net ionization rate of the gas.

The corona-induced decomposition of SF_6 was monitored periodically with a gas chromatograph-mass spectrometer. When SF_6 was degraded by corona at a constant level of 2.0 μA for about a day (24 hours), the primary detectable decomposition products were H_2O and the oxyfluorides SOF_2 and SO_2F_2. The existence of these also imply the presence of HF and SF_4 which could not be detected with the procedures used. After much longer times, there was also evidence of other gaseous species such as SO_2, OCS, CO, and CO_2. The concentrations of SOF_2 and SO_2F_2 after 24 hours were, respectively, at the 10 and 30 ppm levels. The H_2O is apparently driven from the electrodes due to heating by the discharge. It would appear from these studies that, unless precautions are taken to precondition electrodes such as by extensive baking under vacuum, it is impossible to avoid introducing H_2O when operating a corona discharge. The H_2O content appears to level off after the first 10 to 20 hours of operation. The pulse burst characteristics of corona show a dramatic change after 4 hours of corona, thus suggesting that these are significantly affected by decomposition products present at only the ppm level.

The questions of defining and measuring corona inception voltages in SF_6 under dc and 60-Hz ac conditions were also addressed. The technique employed here was one of measuring pulse counts versus applied voltage (peak voltage in the case of 60 Hz). It was found that dc measurements of inception do not always give a good indication of what will happen under 60-Hz ac conditions,

particularly at gas pressures above 200 kPa. Although the ac and dc negative inceptions are close in value, the positive inceptions may differ by nearly as much as a factor of 2.0 at 500 kPa. This difference can be explained in terms of the build up of negative ion space charge in the gap under ac voltage. The dc inceptions are also affected more by the presence of uv radiation in the gap.

In summary, the results of the laboratory measurements reported here help provide a better fundamental understanding of corona phenomena in compressed gaseous dielectrics. The measurement techniques developed will be useful in further studies of corona and should be helpful in designing tests to evaluate relative performance of various new dielectric gases. With the methods considered one can gain a better understanding of processes leading to aging or deterioration of the insulation. The information acquired may also aid in design of techniques to monitor and predict insulation aging in practical systems.

As an aid to those involved with theoretical prediction of breakdown and modeling of discharges in gaseous dielectrics we have prepared an extensive bibliography of electron swarm data. We have also compiled and evaluated the existing swarm data which is likely to be most relevant to dielectrics research.

References

1. R. J. Van Brunt and M. Misakian, "Comparison of DC and 60-Hz AC Positive and Negative Partial Discharge Inceptions in SF_6," Proc. Conf. on Electrical Insulation and Dielectric Phenomena, National Academy of Sciences Press, Boston (1980).
2. R. J. Van Brunt, J. S. Hilten, D. P. Silver, "Partial-Discharge Pulse Height Distributions and Frequencies for Positive and Negative DC Corona in SF_6 and SF_6-N_2 Mixtures," Gaseous Dielectrics II, Proceedings of the Second International Symposium on Gaseous Dielectrics, Pergamon Press, pp. 303-311 (1980).
3. D. A. Leep and R. J. Van Brunt, "Pulse Characteristics of Positive DC Corona in SF_6: Effects of Trace Decomposition Products," Proc. 33rd Gaseous Electronics Conference, to be published in Bull. Am. Phys. Soc. (1980).
4. E. Beaty, J. Dutton and L. Pitchford, "Electron Swarm Data Relevant to High-Voltage Insulation," Gaseous Dielectrics II, Proceedings of the Second International Symposium on Gaseous Dielectrics, Pergamon Press, pp. 25-31 (1980).
5. E. C. Beaty, J. Dutton, L. C. Pitchford, "A Bibliography of Electron Swarm Data," JILA Information Center Report No. 20, Univ. of Colorado (1979).
6. R. J. Van Brunt, "Minutes of Workshop on Gaseous Dielectrics for Use in Future Electric-Power Systems," U.S. National Bureau of Standards Interagency Report, NBSIR 80-1966 (1980).

7. D. A. Leep and R. J. Van Brunt, "Safety Considerations for Handling SF_6 Used in Electrical Equipment," U.S. National Bureau of Standards Interagency Report, NBSIR 80-2063 (1980).

8. A. H. Cookson and R. E. Wootton, "AC Corona and Breakdown Characteristics for Rod Gaps in Compressed Hydrogen, SF_6 and Hydrogen-SF_6 Mixtures," IEEE Trans. Power App. Syst., Vol. PAS-97, pp. 415-422, (1978).

9. O. Farish, O. E. Ibrahim, and A. Kurimoto, "Prebreakdown Corona in SF_6 and SF_6/N_2 Mixtures," 3rd Int. Symp. on High Voltage Eng., Milan, (1979).

10. R. Hazel and E. Kuffel, "Static Field Anode Corona Characteristics in Sulfur Hexafluoride," IEEE Trans. Power App. Syst., Vol. PAS-95, pp. 178-185 (1976).

11. O. Ibrahim, "Corona Stabilization and Breakdown in SF_6 and SF_6/N_2 Mixtures," Ph. D. Thesis, University of Strathclyde, Glasgow, Scotland, (1980).

12. R. Bartnikas, "Use of Multi-channel Analyzer for Corona Pulse-Height Distribution Measurements on Cables and Other Electrical Apparatus," IEEE Trans. Instru. and Meas., Vol. IM-22, pp. 403-407 (1973).

13. R. Bartnikas, "Note on Multi-Channel Corona Pulse-Height Analysis," IEEE Trans. Electr. Insul., Vol. EI-8, pp. 2-5 (1973).

14. K. N. Mathes, "Monitoring Voltage Aging in Liquid Impregnated Solids with Pulse Analysis," Proc. EPRI Seminar on Solid Dielectric Materials Applied to the Electric Power Industry, Monterey, CA (1979).

15. R. Bartnikas, "Corona Pulse Counting and Pulse Height Analysis Techniques," in Engineering Dielectrics I, Corona Measurement and Interpretation, American Society for Testing and Materials, Philadelphia, (1979).

16. W. E. Anderson and R. S. Davis, "Measurements on Insulating Materials at Cryogenic Temperatures," Final Report, U.S. National Bureau of Standards Interagency Report, NBSIR 79-1950 (1980).

17. L. B. Loeb, Electrical Coronas - Their Basic Physical Mechanisms, University of California Press, (1965).

18. W. F. Schmidt, H. Jungblut, D. Hansen and H. Tagashira," Ionic and Electronic Processes in Sulfur Hexafluoride," Gaseous Dielectrics II, Proceedings of the Second International Symposium on Gaseous Dielectrics, Pergamon Press, pp. 1-11 (1980); W. F. Schmidt and H. Jungblut, "Ion Mobility and Recombination in Compressed Sulfur Hexafluoride," J. Phys. D: Appl. Phys. Vol. 12, pp. L67-L70 (1979).

19. P. L. Patterson, "Mobilities of Negative Ions in SF_6," J. Chem. Phys. 53, p. 696 (1970)

20. N. H. Malik and A. H. Qureshi, "The Influence of Voltage Polarity and Field Non-Uniformity on the Breakdown Behavior of Rod-Plane Gaps Filled with SF_6," Trans. Electr. Insul., Vol. EI-14, pp. 327-333.

21. E. Weber, Electromagnetic Theory, Dover, New York, p. 509 (1965).

22. C. C. Bondene, J. Cluet, G. Keib, and G. Wind," Identification and Study of Some Properties of Compounds Resulting from the Decomposition of SF_6 Under the Effect of Electrical Arcing in Circuit-Breakers," Revue Generale De L'Electricite (RGE)-Numero Special, pp. 45-78 (1974).

23. K. Hirooka, H. Kuwahara, M. Noshiro and Y. Jitsugiri, "Decomposition Products of SF_6 Gas by High-Current Arc and Their Reaction Mechanism," Elec. Eng. in Japan, Vol. 95, No. 6 (1975).

24. S. Tominaga, H. Kuwahara, and K. Hirooka, "Influence of Arc-Decomposed Gas on Cast Epoxy Insulators for Gas Insulated Switchgear," IEEE Trans. Power Apparatus and Systems, Vol. PAS-98, No. 6, pp. 2107-2114 (1979).

25. J. Castonquay, A. Theoret and R. Gilbert, "Arc Degradation of SF_6 in the Presence of Polymeric Insulating Materials," Conference Record of 1978, IEEE International Symposium on Electrical Insulation, Philadelphia, pp. 162-166 (1978).

26. T. Suzuki, S. Nakayama and T. Yoshimitsu, "Degradation of Insulating Materials, Due to SF_6 Gas Dissociation Products," IEEE Trans. on Elec. Insul., Vol. EI-15, No. 1, pp. 53-58 (1980).

27. A. K. Vijh, "Nature of Metal-Electrodes/SF_6 Reactions in SF_6 Decomposition Due to Direct-Current Interruption Under Simulated Circuit-Breaker Conditions," IEEE Trans. on Elec. Insul., Vol. EI-11, No. 4, pp. 157-160 (1976).

28. W. Becher and J. Massonne, "Contribution to the Decomposition of Sulfur Hexafluoride in Electric Arcs and Sparks," Elektrotech. Z., Vol. A91, pp. 605-610 (1970).

29. To our knowledge the only published work on degradation of SF_6 in corona is by B. Burta'kova', J. Krump and V. Voshlik, Electrotechnicky Obzor, Prague 67, p. 230 (1978).

30. Certain commercial equipment, instruments or materials are identified in this report in order to adequately specify the experimental procedure. In no case does such identification imply recommendation or endorsement by the National Bureau of Standards, nor does it imply that the material or equipment identified is necessarily the best available for the purpose.

31. I. Sauers, T. J. Havens and L. G. Christophorou," Carbon Inhibition in Sparked Perfluorocarbon - SF_6 Mixtures," J. Phys. D: Appl. Phys., Vol. 13, pp. 1283-90 (1980).

32. K. C. Smyth and P. K. Schenck, "Opto-Galvanic Spectroscopy of Neon Discharges: Mechanism Studies," Chem. Phys. Letters, Vol. 55, pp. 466-472 (1978).

33. D. Feldman, "Opto-galvanic Spectroscopy of Some Molecules in Discharges: NH_2, NO_2, and N_2," Opt. Comm., Vol. 24, pp. 67-72 (1979).

34. W. C. Bridges, "Characteristics of an Opto-galvanic Effect in Cesium and Other Gas Discharge Plasma," J. Opt. Soc. Am., Vol. 68, pp. 352-357 (1978).

NBS-114A (REV. 2-8C)

U.S. DEPT. OF COMM. **BIBLIOGRAPHIC DATA SHEET** *(See instructions)*	1. PUBLICATION OR REPORT NO. NBSIR 81-2242	2. Performing Organ. Report No.	3. Publication Date

4. TITLE AND SUBTITLE

1980 Annual Report: Technical Assistance for Future Insulation Systems Research

5. AUTHOR(S)

R. J. Van Brunt, M. Misakian, D. A. Leep, K. J. Moy, and E. C. Beaty

6. PERFORMING ORGANIZATION *(If joint or other than NBS, see instructions)*

NATIONAL BUREAU OF STANDARDS
DEPARTMENT OF COMMERCE
WASHINGTON, D.C. 20234

7. Contract/Grant No.
EA-77-01-6010
Task No. A053-EES

8. Type of Report & Period Covered

Annual Report 1980

9. SPONSORING ORGANIZATION NAME AND COMPLETE ADDRESS *(Street, City, State, ZIP)*

Department of Energy
Office of Electric Energy Systems
Washington, D.C. 20461

10. SUPPLEMENTARY NOTES

☐ Document describes a computer program; SF-185, FIPS Software Summary, is attached.

11. ABSTRACT *(A 200-word or less factual summary of most significant information. If document includes a significant bibliography or literature survey, mention it here)*

An experimental technique has been developed to quantify the electrical characteristics of pulse-type partial discharges (corona) in compressed electronegative gases. By this method the pulse repetition rates, shapes, and height distributions are determined together with the average current. The technique has been applied to the investigation of corona behavior in compressed SF_6 and SF_6/N_2 mixtures, and to measurements of corona inceptions in SF_6 for both dc and 60-Hz ac voltages. A gas chromatograph-mass spectrometer has been employed to monitor production of trace contaminants by corona-induced degradation of SF_6. The most abundant gaseous by-products that were detected from dc corona were H_2O, SOF_2, and SO_2F_2. The results of chemical analysis were correlated with measurements of the electrical characteristics of the corona and it was discovered that the pulse height distributions and repetition rates were sensitive to the presence of trace contaminants at the ppm level. Experiments were also performed on the effect of trace levels of water vapor, introduced by heating a wire, on positive dc corona pulse burst behavior in SF_6. It was noted that the burst activity was significantly inhibited by trace amounts of H_2O. These results indicate that measurement of pulse characteristics of positive corona can be used as a sensitive monitor of gaseous contamination levels. The effects of uv radiation and optical radiation from a tunable dye laser on electrical behavior of corona in SF_6 and N_2 were investigated. Ultra-violet light can have, under certain conditions, a large effect on initiation of electron avalanches in SF_6 near onset. Optical radiation in the wavelength range 580 to 620 nm was found to produce a measurable effect on corona in N_2 when it impinged on the electrode surfaces. A bibliography of electron swarm data needed to predict theoretically breakdown and to model discharge phenomena in gases was prepared.

12. KEY WORDS *(Six to twelve entries; alphabetical order; capitalize only proper names; and separate key words by semicolons)*

corona; decomposition; electrical insulation; gas chromatograph; inception voltages; mass spectrometer; partial discharge; sulfur hexafluoride; swarm data; water vapor

13. AVAILABILITY

☒ Unlimited

☐ For Official Distribution. Do Not Release to NTIS

☐ Order From Superintendent of Documents, U.S. Government Printing Office, Washington, D.C. 20402.

☒ Order From National Technical Information Service (NTIS), Springfield, VA. 22161

14. NO. OF PRINTED PAGES

15. Price